

POLYTECHNIC OF TURIN

Master's degree in civil engineering



Master's degree thesis

**Risk assessment of bridge's piers subjected
to multiple earthquakes: comparison
between different approaches.**

Relatori

Prof. Paolo Castaldo

Prof. Enrico Tubaldi

Candidato

Deborah Di Pilato

matricola 241816

A.A. 2018/2019

TABLE OF CONTENTS

TABLE OF CONTENTS	2
ACKNOWLEDGEMENTS	4
SUMMARY	5
LIST OF TABLES.....	6
LIST OF FIGURES	7
1 INTRODUCTION	10
1.1 Background	10
1.2 Research Objective and Scope	11
1.3 Outline of the Thesis.....	12
2 ENGINEERING DEMAND PARAMETERS AND DAMAGE INDEX.....	13
2.1 Global EDP: Park and Ang damage index.....	14
2.2 Local EPDs.....	15
3 OVERVIEW OF THE STOCHASTIC APPROACHES FOR THE EVALUATION OF LIFETIME MAIN-SHOCK HAZARD.....	17
3.1 Risk assessment.....	17
3.2 Ghosh et al. Method	18
3.2.1 Modified regression model.....	19
3.2.2 Exceedance probability.....	20
3.3 Iervolino et al. Method	21
3.3.1 Markov-type seismic damage accumulation process.....	21
3.4 Frequentist probability.....	26
4 STRUCTURAL MODELS.....	27
4.1 Introduction	27
4.2 Finite element model of RC bridge columns	27
4.3 Materials.....	30
4.3.1 Confined and unconfined concrete model	30
4.3.2 Reinforcing steel model	31
4.3.3 Low-cycle fatigue degradation model.....	32
4.3.4 Bond-slip displacement model for zero length element	33
5 ILLUSTRATIVE APPLICATIONS OF THE THREE METHODS TO THE MODELS....	37

5.1	Introduction	37
5.2	Ground motion selection.....	38
5.3	Results of Lehman and Mohel column 815	40
5.3.1	Ghosh et a. model.....	40
5.3.2	Hybrid method.....	68
5.3.3	Comparison between different approaches.....	68
5.4	Results of Lehman and Mohel column 1015	71
5.4.1	Ghosh et al. model	71
5.4.2	Comparison between different approaches.....	96
6	CONCLUSIONS.....	98
	BIBLIOGRAPHY.....	101

ACKNOWLEDGEMENTS

A special thanks to the professor Paolo Castaldo, for giving me the opportunity to have the experience in Scotland, for having pushed me beyond my limits and for the ongoing support. You are the most smiling and obliging professor I have ever met. Thanks for everything.

I cannot omit to thank Enrico Tubaldi, a brilliant professor completely in love with his work. Thank you for having followed me constantly throughout my stay in Scotland. I hope one day to be as passionate about my work as you.

Thanks also to Diego Gino, the most helpful and kind PHD of Polito for having solved all my doubts before the exams.

A huge thanks to my wonderful family, without which I could not live, and to my precious friends who make my life more cheerful and carefree. I love you so much.

SUMMARY

Frequently, buildings and infrastructures are in regions prone to earthquake excitations. These structures are continuously exposed to main-shock earthquakes throughout their lifetime. Repeated shocks can cause a strong reduction of structural capacity leading to collapse and, as consequence, to a devastating impact on the urban context in terms of both human losses and economic stability.

Considering the prospect of potential future destructive events, risk assessment has to focus on probabilistic models able to best predict future scenarios and consider the high uncertainties involved in the analysis.

The present study proposes a comparison between three probabilistic approaches for the seismic risk estimation of different bridge piers. In the all three methods, the probability of occurrence related to seismic main-shocks as well as the effects induced on the structure are evaluated separately by applying the total probability theorem. In the first one, conceived by Ghosh et al. (2015), the accumulation of damage is based on predictive regression models. Whereas, Iervolino et al. (2015) describe the progressive structural degradation using a homogeneous Markov process in discrete time. The last methodology includes the seismic risk assessment through the classic frequentist approach. The results deriving from the above-mentioned methods are described, compared and finally discussed.

LIST OF TABLES

TABLE 1. DAMAGE LEVEL CLASSIFICATION AND CORRELATION WITH CALCULATED DAMAGE INDICES AND DAMAGE MEASURES.....	15
TABLE 2 ULTIMATE VALUE FOR LOCAL EDPs.....	16
TABLE 3. DETAILS OF COLUMN DATASET.....	28
TABLE 4 INPUT DATA FOR GROUND MOTION GENERATION.....	38
TABLE 5 STRUCTURAL CHARACTERISTIC FOR COLUMN 815.....	40
TABLE 6 REGRESSION COEFFICIENT AND RESPECTIVE RMSE.....	42
TABLE 7 REGRESSION COEFFICIENT AND RESPECTIVE RMSE.....	44
TABLE 8 REGRESSION COEFFICIENT AND RESPECTIVE RMSE.....	49
TABLE 9 REGRESSION COEFFICIENTS AND RESPECTIVE RMSE.....	50
TABLE 10 REGRESSION COEFFICIENTS AND RESPECTIVE RMSE.....	54
TABLE 11 MULTILINEAR REGRESSION MODEL FOR PREDICTING THE DAMAGE INDEX AFTER N SHOCKS AS A FUNCTION OF THE PGA OF THE NTH SHOCK AND THE DAMAGE INDEX OF THE PREVIOUS ONE. REGRESSION IS CARRIED OUT WITH AN INCREASING NUMBER OF SAMPLES A)300 B)1000 C)2500 D)3500.....	55
TABLE 12 REGRESSION COEFFICIENTS AND RESPECTIVE RSME.....	55
TABLE 13 REGRESSION COEFFICIENTS AND RESPECTIVE RMSE.....	59
TABLE 14 REGRESSION COEFFICIENTS AND RESPECTIVE RMSE.....	60
TABLE 15 REGRESSION COEFFICIENTS AND RMSE.....	64
TABLE 16 REGRESSION COEFFICIENTS AND RMSE.....	65
TABLE 17 STRUCTURAL CHARACTERISTIC FOR COLUMN 1015.....	71
TABLE 18 REGRESSION COEFFICIENTS AND RMSE.....	72
TABLE 19 REGRESSION COEFFICIENTS AND RMSE.....	73
TABLE 20 REGRESSION COEFFICIENTS AND RMSE.....	77
TABLE 21 REGRESSION COEFFICIENTS AND RMSE.....	78
TABLE 22 REGRESSION COEFFICIENTS AND RMSE.....	82
TABLE 23 REGRESSION COEFFICIENTS AND RMSE.....	83
TABLE 24 REGRESSION COEFFICIENTS AND RMSE.....	87
TABLE 25 REGRESSION COEFFICIENTS AND RMSE.....	88
TABLE 26 REGRESSION COEFFICIENTS AND RMSE.....	92
TABLE 27 REGRESSION COEFFICIENTS AND RMSE.....	93

LIST OF FIGURES

FIGURE 2.1. SECTION OF A FIBRE BEAM-COLUMN ELEMENT, WE CAN DISTINGUISH 3 ELEMENTS: A) STEEL REINFORCEMENT IN RED; B) UNCONFINED CONCRETE IN WITHE C) CONFINED CONCRETE IN GREY.	16
FIGURE 3.1 COMPARISON BETWEEN GHOSH METHOD AND GHOSH MODIFIED.	20
FIGURE 3.2. SCHEME OF DEGRADATION STATES OF A DAMAGE-ACCUMULATING STRUCTURE.	23
FIGURE 4.1 SCHEMATIC VIEW OF THE EXPERIMENTAL UNITS TESTED BY LEHMAN AND MOEHLE (2000) ...	28
FIGURE 4.2 SCHEMATIZATION OF A FIBRE BEAM-COLUMN ELEMENT WITH BAR BUCKLING AND BAR SLIP MODEL.	29
FIGURE 4.3 CYCLIC RESPONSE OF CONCRETE MODEL EMPLOYED IN THE ANALYSES: (A) UNCONFINED AND CONFINED CONCRETE RESPONSE IN COMPRESSION INCLUDING CYCLIC RESPONSE; (B) TENSION.	31
FIGURE 4.4 DHAKAL AND MAEKAWA BUCKLING MODEL.	32
FIGURE 4.5 FATIGUE MATERIAL REGRESSION MODEL TO PREDICTING THE FRACTURE OF REINFORCEMENT DUE TO LOW-CYCLE FATIGUE.....	33
FIGURE 4.6 BAR SLIP MODEL	34
FIGURE 4.7 BAR STRESS-SLIP MODEL USED IN ZERO LENGTH SECTION.	35
FIGURE 4.8 ASSUMED COMPRESSIVE DEPTH	36
FIGURE 4.9 STRESS-SLIP MODEL	36
FIGURE 5.1 RAPRESENTATION OF MULTIPLE EARTHQUAKE.....	39
FIGURE 5.2 LINEAR REGRESSION MODEL FOR PREDICTING THE DAMAGE INDEX FOLLOWING SINGLE SHOCK. REGRESSION IS CARRIED OUT WITH AN INCREASING NUMBER OF SAMPLES A)300 B)1000 C)2500 D)3500.....	41
FIGURE 5.3 MULTILINEAR REGRESSION MODEL FOR PREDICTING THE DAMAGE INDEX AFTER N SHOCKS AS A FUNCTION OF THE PGA OF THE NTH SHOCK AND THE DAMAGE INDEX OF THE PREVIOUS ONE. REGRESSION IS CARRIED OUT WITH AN INCREASING NUMBER OF SAMPLES A)300 B)1000 C)2500 D)3500.....	43
FIGURE 5.4 PROBABILITY OF FAILURE WITH AN INCREASING NUMBER OF OCCURRENCES.....	45
FIGURE 5.5 PROBABILITY OF FAILURE EVALUATED WITH AN INCREASING NUMBER OF SAMPLES	46
FIGURE 5.6 CYCLIC RESPONSE OF CONFINED CONCRETE MODEL UNDER COMPRESSION, EMPLOYED IN THE ANALYSES.....	47
FIGURE 5.7 LINEAR REGRESSION MODEL FOR PREDICTING THE DAMAGE INDEX FOLLOWING SINGLE SHOCK. REGRESSION IS CARRIED OUT WITH AN INCREASING NUMBER OF SAMPLES A)300 B)1000 C)2500 D)3500.....	48
FIGURE 5.8 MULTILINEAR REGRESSION MODEL FOR PREDICTING THE DAMAGE INDEX AFTER N SHOCKS AS A FUNCTION OF THE PGA OF THE NTH SHOCK AND THE DAMAGE INDEX OF THE PREVIOUS ONE. REGRESSION IS CARRIED OUT WITH AN INCREASING NUMBER OF SAMPLES A)300 B)1000 C)2500 D)3500.....	50
FIGURE 5.9 PROBABILITY OF FAILURE WITH AN INCREASING NUMBER OF OCCURRENCES.....	51
FIGURE 5.10 PROBABILITY OF FAILURE EVALUATED WITH AN INCREASING NUMBER OF SAMPLES.	52
FIGURE 5.11 CYCLIC RESPONSE OF UNCONFINED CONCRETE MODEL UNDER COMPRESSION, EMPLOYED IN THE ANALYSES.....	53
FIGURE 5.12 LINEAR REGRESSION MODEL FOR PREDICTING THE DAMAGE INDEX FOLLOWING SINGLE SHOCK. REGRESSION IS CARRIED OUT WITH AN INCREASING NUMBER OF SAMPLES A)300 B)1000 C)2500 D)3500.....	54
FIGURE 5.13 PROBABILITY OF FAILURE WITH AN INCREASING NUMBER OF OCCURRENCES.....	56
FIGURE 5.14 PROBABILITY OF FAILURE EVALUATED WITH AN INCREASING NUMBER OF SAMPLES.	57
FIGURE 5.15 CYCLIC RESPONSE OF UNCONFINED CONCRETE MODEL UNDER TENSION, EMPLOYED IN THE ANALYSES.....	58
FIGURE 5.16 LINEAR REGRESSION MODEL FOR PREDICTING THE DAMAGE INDEX FOLLOWING SINGLE SHOCK. REGRESSION IS CARRIED OUT WITH AN INCREASING NUMBER OF SAMPLES A)300 B)1000 C)2500 D)3500.....	59

FIGURE 5.17 MULTILINEAR REGRESSION MODEL FOR PREDICTING THE DAMAGE INDEX AFTER N SHOCKS AS A FUNCTION OF THE PGA OF THE NTH SHOCK AND THE DAMAGE INDEX OF THE PREVIOUS ONE. REGRESSION IS CARRIED OUT WITH AN INCREASING NUMBER OF SAMPLES A)300 B)1000 C)2500 D)3500.....	60
FIGURE 5.18 PROBABILITY OF FAILURE WITH AN INCREASING NUMBER OF OCCURRENCES.....	61
FIGURE 5.19 PROBABILITY OF FAILURE EVALUATED WITH AN INCREASING NUMBER OF SAMPLES.....	62
FIGURE 5.20 CYCLIC RESPONSE OF STEEL REINFORCEMENT MODEL UNDER COMPRESSION, EMPLOYED IN THE ANALYSES.....	63
FIGURE 5.21 LINEAR REGRESSION MODEL FOR PREDICTING THE DAMAGE INDEX FOLLOWING SINGLE SHOCK. REGRESSION IS CARRIED OUT WITH AN INCREASING NUMBER OF SAMPLES A)300 B)1000 C)2500 D)3500.....	64
FIGURE 5.22 MULTILINEAR REGRESSION MODEL FOR PREDICTING THE DAMAGE INDEX AFTER N SHOCKS AS A FUNCTION OF THE PGA OF THE NTH SHOCK AND THE DAMAGE INDEX OF THE PREVIOUS ONE. REGRESSION IS CARRIED OUT WITH AN INCREASING NUMBER OF SAMPLES A)300 B)1000 C)2500 D)3500.....	65
FIGURE 5.23 PROBABILITY OF FAILURE WITH AN INCREASING NUMBER OF OCCURRENCES.....	66
FIGURE 5.24 PROBABILITY OF FAILURE EVALUATED WITH AN INCREASING NUMBER OF SAMPLES.....	67
FIGURE 5.25 PROBABILITY OF FAILURE EVALUATED WITH DIFFERENT APPROACHES: GHOSH METHOD, IERVOLINO METHOD, FREQUENTIST APPROACH AND HYBRID ONE FOR THE CHOSEN EPDs (A) PARK AND ANG INDEX, B) STRAIN OF CONFINED CONCRETE UNDER COMPRESSION C) STRAIN OF UNCONFINED CONCRETE UNDER COMPRESSION AND D)TENSION AND E) STRAIN OF STEEL UNDER COMPRESSION) ..	70
FIGURE 5.26 LINEAR REGRESSION MODEL FOR PREDICTING THE DAMAGE INDEX FOLLOWING SINGLE SHOCK. REGRESSION IS CARRIED OUT WITH AN INCREASING NUMBER OF SAMPLES A)300 B)1000 C)2500 D)3500.....	72
FIGURE 5.27 MULTILINEAR REGRESSION MODEL FOR PREDICTING THE DAMAGE INDEX AFTER N SHOCKS AS A FUNCTION OF THE PGA OF THE NTH SHOCK AND THE DAMAGE INDEX OF THE PREVIOUS ONE. REGRESSION IS CARRIED OUT WITH AN INCREASING NUMBER OF SAMPLES A)300 B)1000 C)2500 D)3500.....	73
FIGURE 5.28 PROBABILITY OF FAILURE WITH AN INCREASING NUMBER OF OCCURRENCES.....	74
FIGURE 5.29 PROBABILITY OF FAILURE EVALUATED WITH AN INCREASING NUMBER OF SAMPLES.	75
FIGURE 5.30 CYCLIC RESPONSE OF CONFINED CONCRETE MODEL UNDER COMPRESSION, EMPLOYED IN THE ANALYSES.....	76
FIGURE 5.31 LINEAR REGRESSION MODEL FOR PREDICTING THE DAMAGE INDEX FOLLOWING SINGLE SHOCK. REGRESSION IS CARRIED OUT WITH AN INCREASING NUMBER OF SAMPLES A)300 B)1000 C)2500 D)3500.....	77
FIGURE 5.32 MULTILINEAR REGRESSION MODEL FOR PREDICTING THE DAMAGE INDEX AFTER N SHOCKS AS A FUNCTION OF THE PGA OF THE NTH SHOCK AND THE DAMAGE INDEX OF THE PREVIOUS ONE. REGRESSION IS CARRIED OUT WITH AN INCREASING NUMBER OF SAMPLES A)300 B)1000 C)2500 D)3500.....	78
FIGURE 5.33 PROBABILITY OF FAILURE WITH AN INCREASING NUMBER OF OCCURRENCES.....	79
FIGURE 5.34 PROBABILITY OF FAILURE EVALUATED WITH AN INCREASING NUMBER OF SAMPLES.	80
FIGURE 5.35 CYCLIC RESPONSE OF UNCONFINED CONCRETE MODEL UNDER COMPRESSION, EMPLOYED IN THE ANALYSES.....	81
FIGURE 5.36 LINEAR REGRESSION MODEL FOR PREDICTING THE DAMAGE INDEX FOLLOWING SINGLE SHOCK. REGRESSION IS CARRIED OUT WITH AN INCREASING NUMBER OF SAMPLES A)300 B)1000 C)2500 D)3500.....	82
FIGURE 5.37 MULTILINEAR REGRESSION MODEL FOR PREDICTING THE DAMAGE INDEX AFTER N SHOCKS AS A FUNCTION OF THE PGA OF THE NTH SHOCK AND THE DAMAGE INDEX OF THE PREVIOUS ONE. REGRESSION IS CARRIED OUT WITH AN INCREASING NUMBER OF SAMPLES A)300 B)1000 C)2500 D)3500.....	83
FIGURE 5.38 PROBABILITY OF FAILURE WITH AN INCREASING NUMBER OF OCCURRENCES.....	84
FIGURE 5.39 PROBABILITY OF FAILURE EVALUATED WITH AN INCREASING NUMBER OF SAMPLES.	85

FIGURE 5.40 CYCLIC RESPONSE OF UNCONFINED CONCRETE MODEL UNDER TENSION, EMPLOYED IN THE ANALYSES.....	86
FIGURE 5.41 LINEAR REGRESSION MODEL FOR PREDICTING THE DAMAGE INDEX FOLLOWING SINGLE SHOCK. REGRESSION IS CARRIED OUT WITH AN INCREASING NUMBER OF SAMPLES A)300 B)1000 C)2500 D)3500.....	87
FIGURE 5.42 MULTILINEAR REGRESSION MODEL FOR PREDICTING THE DAMAGE INDEX AFTER N SHOCKS AS A FUNCTION OF THE PGA OF THE NTH SHOCK AND THE DAMAGE INDEX OF THE PREVIOUS ONE. REGRESSION IS CARRIED OUT WITH AN INCREASING NUMBER OF SAMPLES A)300 B)1000 C)2500 D)3500.....	88
FIGURE 5.43 PROBABILITY OF FAILURE WITH AN INCREASING NUMBER OF OCCURRENCES.....	89
FIGURE 5.44 PROBABILITY OF FAILURE EVALUATED WITH AN INCREASING NUMBER OF SAMPLES	90
FIGURE 5.45 CYCLIC RESPONSE OF STEEL REINFORCEMENT MODEL UNDER COMPRESSION, EMPLOYED IN THE ANALYSES.....	91
FIGURE 5.46 LINEAR REGRESSION MODEL FOR PREDICTING THE DAMAGE INDEX FOLLOWING SINGLE SHOCK. REGRESSION IS CARRIED OUT WITH AN INCREASING NUMBER OF SAMPLES A)300 B)1000 C)2500 D)3500.....	92
FIGURE 5.47 MULTILINEAR REGRESSION MODEL FOR PREDICTING THE DAMAGE INDEX AFTER N SHOCKS AS A FUNCTION OF THE PGA OF THE NTH SHOCK AND THE DAMAGE INDEX OF THE PREVIOUS ONE. REGRESSION IS CARRIED OUT WITH AN INCREASING NUMBER OF SAMPLES A)300 B)1000 C)2500 D)3500.....	93
FIGURE 5.48 PROBABILITY OF FAILURE WITH AN INCREASING NUMBER OF OCCURRENCES.....	94
FIGURE 5.49 PROBABILITY OF FAILURE EVALUATED WITH AN INCREASING NUMBER OF SAMPLES.	95
FIGURE 5.50 PROBABILITY OF FAILURE EVALUATED WITH DIFFERENT APPROACHES: GHOSH METHOD, IERVOLINO METHOD, FREQUENTIST APPROACH AND HYBRID ONE FOR THE CHOSEN EPDS (A) PARK AND ANG INDEX, B) STRAIN OF CONFINED CONCRETE UNDER COMPRESSION C) STRAIN OF UNCONFINED CONCRETE UNDER COMPRESSION AND D)TENSION AND E) STRAIN OF STEEL UNDER COMPRESSION)..	97

1 INTRODUCTION

1.1 Background

Around the globe, many critical infrastructure elements, such as strategic buildings or highway bridges, are in regions inclined to earthquake excitations. Past catastrophic events, such as the 1971 San Fernando earthquake and the more recent ones the 1994 Northridge earthquake, have demonstrated that bridges are one of the most vulnerable components of transportation systems. Exposure to repeated quake pulses may lead to damage accumulation, eventually causing exceedance of limiting threshold capacity and imminent structural collapse. (J. Ghosh, 2015) By way of example, a study of the Californian OES (Office Emergency Services) reports that the 1994 Northridge earthquake caused 57 casualties, 10,000 injuries and extensive damages to infrastructures and households throughout the county of Los Angeles and surrounding valleys worth \$ 46,000 million. Primarily because of the importance of the dealt topics, there is an increasing interest in the life-cycle analysis of civil constructions that requires the modelling of structural performance across the service life. In that sense, seismic risk assessment has a central role and it need to be in the same time prospective and scientifically credible.

The Seismic risk is the probability of losses occurring due to earthquakes in a given period in terms of human lives, social disruption as well as economic one. Hence a qualitative definition

$$\text{SEISMIC RISK} = \text{SEISMIC HAZARD} \bullet \text{VULNERABILITY} \bullet \text{EXPOSURE}$$

Seismic Hazard is dependent on the characteristics of the physical event and the geological characteristics of the area in which the event occurs: the greater the frequency and intensity of the events

that characterize a geographical area, the greater its danger. In a rigorous way it could be evaluated as the level of damage caused by the seism and the corresponding probability of its occurrence. Vulnerability is connected to the susceptibility of the structure to suffer when exposed to a quake effect in terms of potential life and economic loss. Exposure is a quantification of the potential losses and so density of people and buildings, number of commercial activity, the amount and type of important infrastructure and buildings concentrated in the area assessed.

The assess of seismic risk require seismological and engineering bases in order to formulate earthquake prediction models which permit to assess the risk of loss as a result of a catastrophic event and so the estimation of seismic damage.

1.2 Research Objective and Scope

The primary focus of the present study is structural damage estimation in reinforced concrete piers under multiple excitations, considering various specific details of the structure including design features and seismic hazard of the site. The FEM model of the piers is used for carrying out the structural analyses that are the basis to realise the hazard assessment. A comparison between three different methods to evaluate structural degradation will be carried out below. To accomplish this objective, the following research tasks have been conducted:

- Critically review current bridge condition assessment procedures
- Application of the previous methodologies mentioned therein to two structural models of bridge's piers with increasing slenderness

- Comparison of the results obtained with the three methodologies in order to establish the advantages and disadvantages of each one

This work aims to evaluate the efficiency of each method in order to establish which is the most advantageous and accurate for the seismic risk assessment.

1.3 Outline of the Thesis

This report is organized in six sections. The second part consists in a description of the Engineering demand parameters chosen for the following analysis. The third part begins with an overview of the three methodologies used for the damage evaluation. Section four presents the analytical models of the bridge piers, calibration of the hysteretic and fatigue model used in the analyses and the process of random generating of the ground motion selection. Then there is a chapter in which the illustrative application of the three methods are shown. Relevant findings from the study and suggestion for additional work are discussed in the final part.

2 ENGINEERING DEMAND PARAMETERS AND DAMAGE INDEX

The extensive injury caused by earthquakes on reinforced concrete structures has shown that they are highly vulnerable to seismic action due to their characteristic low-ductility. This has given impetus to the development of the so-called Performance-based design (PBEE) as a functional tool for risk assessment and the development of retrofitting techniques that reduce structural vulnerability. Therefore, there is the need to use probabilistic demand models to describe the relationship between the structural response and the measurement of the intensity of ground movements (IM). They are widely used in the field of civil engineering, with particular reference to the structures in RC, as they allow us to describe the structural response in terms of engineering demand parameters (*EDPs*).

This latter quantity are indicators used to predict damage to structural and non-structural components and systems. There are two categories of *EDPs*: global and local. The first one describes the general structural behaviour and reduce the computational effort. But, in case of low-ductility structure they can lead to not appropriate or gross results. In this case is better to use local *EDPs* that permits a more realistic description of failure mechanisms for structural vulnerability.

In order to have a good evaluation of the performance of the structural system under seismic pulse it is necessary to choose *EDPs* adequately. In this work probabilistic methods are developed by using the Park and Ang damage index as global *EDP* but, because we are studying a complex model with a high number of degrees of freedoms, it is necessary monitoring also the local response of all structural members. Different *EDPs* are considered in order to highlight the most significant failure

modalities in RC low-ductility structure such as bridge's piers. In the following paragraphs the global and local EPDs used in this work will be illustrated.

2.1 Global EDP: Park and Ang damage index

A large number of damage indices have been proposed in literature, they can be grossly categorized in two main classes: displacement-related and energy-related. **Errore. L'origine riferimento non è stata trovata.** In the first group, the achievement of a certain limit state is due to the exceeding of a maximum displacement threshold and therefore, the maximum deformation. The other one refers to structures in which damaging is linked to the amount of energy dissipated by hysteretic loops. Nevertheless, there are hybrid indices, that captures the combined effect of deformation and dissipated energy demand in order to have a better assessment of the cyclic load effect. The most representative, as well as used for this work, is the Park and Ang damage index. As can be seen from the following formula, it ensues from a linear combination of the maximum deformation induced by the earthquake and the hysteretic energy dissipated. (Park, 1985.)

In terms of damage index this is represented by the following equation

$$D = \frac{u_{max}}{u_u} + \beta \frac{E_h}{F_y u_u}$$

Where D is the Park and Ang damage index, u_{max} is the maximum displacement caused by the earthquake, u_u is the ultimate displacement under monotonic loading, E_h is the total hysteretic energy dissipated, F_y is the yield force, and β is a dimensionless constant usually assumed to be 0.05 for reinforced concrete (RC) structures. (J. Ghosh, 2015)

In order to correlate empirical observed damages with calculated damage indices Park et Ang suggested a classification of damage levels shown below:

Table 1. Damage level classification and correlation with calculated damage indices and damage measures

Level	Damage index (D)	Damage measure
I	$D < 0.1$	No damage, localized minor cracking
II	$0.1 < D < 0.25$	Minor damage; light cracking
III	$0.25 < D < 0.4$	Moderate damage, severe cracking
IV	$0.4 < D < 1$	Severe damage, crushing of concrete
V	$D > 1$	Loss of element load resistance

2.2 Local EPDs

The already mentioned global EDP permits to drastically reduce the computational effort but, its use may lead to incorrect results in the cases of existing low-ductile structures. For this reason, it is necessary to introduce local EPDs. (Freddi, 2016) They are used in order to directly capture the modifications of the frame response and of the capacity induced by low-cycle of fatigue and other non-linear phenomena. To choose the response quantity we analyse the collapse modes of our structure and evaluate the parameters that can cause failure.

In particular, the local EPDs adopted to monitor the seismic demand on the frame due to flexural and axial forces are the maximum-over-time values of:

- the core concrete compressive strain ε_{c_core}
- the cover concrete compressive strain ε_{c_cover}
- the cover concrete tensile strain ε_{t_cover}
- the steel strain ε_s under compression

Table 2 ultimate value for local EDPs.

EDPs	Limit value
ε_{c_core}	0.035
ε_{c_cover}	0.00428
ε_{t_cover}	0.00125
ε_s	0.08

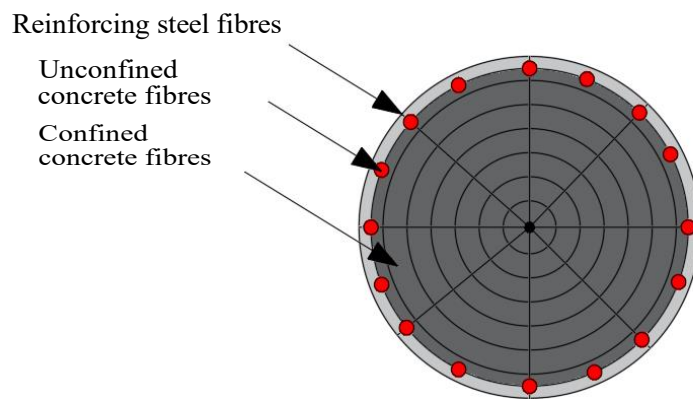


Figure 2.1. Section of a fibre beam-column element, we can distinguish 3 elements: a) steel reinforcement in red; b) unconfined concrete in white c) confined concrete in grey.

3 OVERVIEW OF THE STOCHASTIC APPROACHES FOR THE EVALUATION OF LIFETIME MAIN-SHOCK HAZARD

3.1 Risk assessment

Failure can be interpreted as failure of a system due to exceedance of a limit state or also as failure resulting in the generation of an earthquake. The probability of the generic cumulative engineering demand parameter D , exceeding the value d , can be expressed through total probability theorem as:

$$P[D \geq d] = \sum_{n=1}^{\infty} P[D \geq d | n \text{ shocks}] \cdot P[n, T] \quad (1)$$

Where $P[D \geq d | n \text{ shocks}]$ is the probability that the demand exceeds d , conditional to having n shocks, and $P[n, T]$ is the probability of having n shocks in the design life time T .

The probability of having n shocks in the design life time T can be evaluated based on the mean annual frequency (MAF) of earthquakes of any significant intensity, ν_{eq} , by introducing the Poisson assumption of the occurrence of events:

$$P[n, T] = \frac{(\nu_{eq}T)^n}{n!} e^{-\nu_{eq}T} \quad (2)$$

On the other hand, three different approaches can be employed for evaluating $P[D \geq d | n \text{ shocks}]$, as described below: Ghosh method, Iervolino method and frequentist approach.

3.2 Ghosh et al. Method

This approach focuses on the assessment of damage accumulation under repeated shocks, based on probabilistic regression model, taking into account two possible scenarios: mainshocks and aftershocks. Only the first scenario has been examined in this work.

The use of probabilistic demand models allows us to introduce an approximate function for the structural response. According to Cornell's research, for a single shock event, the relationship between the median structural demand, EDP, and the IM (intensity measure) can be approximated by a power law model (linear model in the log-log space):

$$EDP = a(IM)^b \quad (3)$$

where a and b are regression coefficients.

For structure with nonlinear behaviour, as cases study, the linear regression model in the log-log space could be not valid for the entire IM range of interest. **Errore. L'origine riferimento non è stata trovata.**

Different regression models have been applied to the examined columns, analysing several *EDPs* and finding that a good fit of local *EDPs* such as material stress and strain can be obtained by adopting a bilinear regression. (Freddi, 2016) This is a convenient solution because of its simplicity and the small number of parameters involved in the fitting.

The used regression model is described by the following expression:

$$\ln(D_1) = \alpha_1 + \beta_1 \ln(IM_1) \quad (4)$$

where D_1 is the damage index after the first earthquake pulse, α_1 and β_1 are regression coefficients, and IM_1 is the ground motion intensity of the first earthquake shock.

In case of multiple earthquakes damage index evaluation depends on the history of shock occurrences.

It can be described through a multilinear regression model as follows:

$$\ln(D_n) = \alpha_n + \beta_n \ln(IM_n) + \gamma_n \ln(D_{n-1}) + \delta_n l(IM_n)\ln(D_{n-1}) \quad (5)$$

where D_n is the damage index after the n th earthquake shock with ground motion intensity IM_n ; α_n , β_n , γ_n , and δ_n are regression coefficients; and D_{n-1} is the damage index after $(n - 1)$ earthquake shocks.

This procedure is a sort of extension of the first regression; to apply the equation above the structure has to be subjected to a series of shocks. PGA is chosen as earthquake intensity measure (IM) because of its ability to predict damage index. (J. Ghosh, 2015)

3.2.1 Modified regression model

The nonlinear bridges' behaviour is also expected to induce an increased dispersion of the *EDPs* values, because of the reduced efficiency of an IM that is based on the elastic system properties. To solve these issues and accurately describing the *EDP* a modification in regression model has been introduced. The adjustment takes into account that not all earthquakes cause damage to the structure, this depends on their intensity. Thus, the demand model can be divided in two parts:

$$\log(D_1) = \begin{cases} 0 & IM < IM^* \\ \alpha_n + \beta_n \log(IM_n) & IM \geq IM^* \end{cases} \quad (6)$$

$$\log(D_n) = \begin{cases} \log(D_{n-1}) & IM < IM^* \\ \alpha_n + \beta_n \log(IM_n) + \gamma_n \log(D_{n-1}) + \delta_n \log(IM_n) \log(D_{n-1}) & IM \geq IM^* \end{cases} \quad (7)$$

By introducing this modification, it is possible to improve the regression since the previous model underestimated the damage for

$IM < IM^*$ and overestimated the damage for $IM \geq IM^*$ as we can see in the following figure.

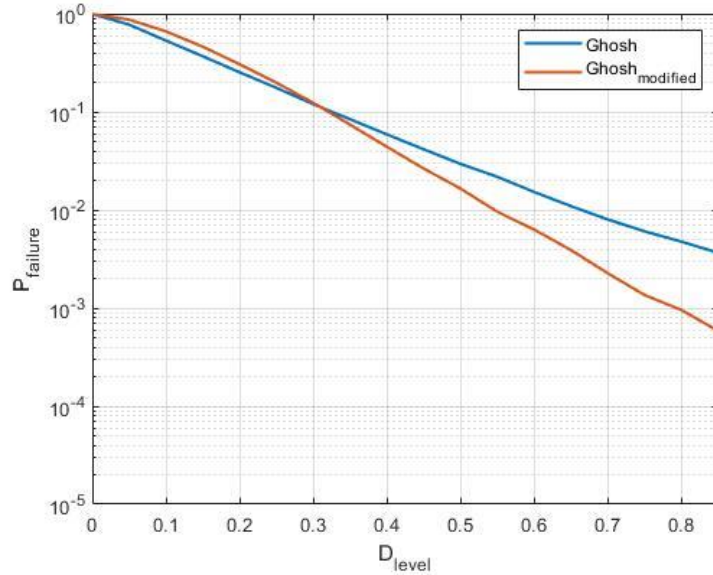


Figure 3.1 Comparison between Ghosh method and Ghosh modified.

3.2.2 Exceedance probability

The chance of exceeding limiting values of the damage index given a time period of interest such as the service life of a structure. Using the total probability theorem, as shown before.

In this case the probability that the demand exceeds a certain level d can be computed as

$$P[D > d | n \text{ shocks}] = \frac{1}{N_{MC}} \sum_i I[D_{ni} > d] \quad (8)$$

where N_{MC} is the total number of Monte Carlo trials, D_{ni} is a realization of the damage index after n shocks for the i th Monte Carlo trial, and $I[\cdot]$ is the indicator function (which equals 1 when $[\cdot]$ is true or 0 if $[\cdot]$ is false).

3.3 Iervolino et al. Method

This study focuses on the stochastic modelling of seismic damage accumulation, as one of the components of life-cycle analysis of structures.

The method is based on the hypothesis that the dependence between the increases of the damage requires that the structural vulnerability, i.e. susceptibility to increase the damage in an earthquake, note the characteristics of the shock, depends only from the state of the structure at the time of the seismism. (Iunio Iervolino, 2015)

The study deals with the stochastic modelling of structures that accumulate seismic damage when the structural fragility is state-dependent, and the hazard is represented by random earthquake occurrence with random intensity.

To describe the degradation considering the vulnerability as a state-dependent phenomenon, a discrete-time homogeneous Markovian process is used. Also, the domain of the structural performance is discretized in terms of several damage states (D) and, given the occurrence of shocks we can derive transition probabilities. The probability of having n shocks in the design life time T is described through a homogeneous Poisson Process, a classical assumption in seismic hazard analysis. To obtain a complete characterization of the damage process we combine the probabilistic description of earthquake occurrence with the transition matrix, that give us the unit-time transition probabilities between states.

3.3.1 Markov-type seismic damage accumulation process

The evaluation of the damage to a structure based on state-dependent vulnerability, by modelling the transition matrix between a DS and the next, allows to predict the behaviour of the already

damaged structure in a probabilistic way and then to predict the structure's path from the first levels of damage up to collapse as the occurrences increase. In this study the progressive damage is modelled by a time-dependent and discrete-state Markovian process in which the time t is discretized in intervals of fixed width equal to Δ , which may be considered to be the time unit (e.g. one year) and the domain of the considered damage index that is the structural performance measure is subdivided in order to have a finite number n of DS. The various D_{Si} , $i = \{1, 2, \dots, n\}$, are the limit states, identifying intervals of the damage metric considered, between as-built conditions and failure, the structure has to walk (not necessarily one-by-one) to reach collapse. (Iunio Iervolino, 2015) Having said that, we can evaluate P_{ij} the transition probabilities between the i -th and j -th generic DS, given the occurrence of an earthquake. These represent the probabilities that after one event the structure pass from the i -th DS (before the shock) to the j -th DS after the earthquake. Arranging P_{ij} in a matrix, which contains probabilities of observing transitions between any possible couple of DS we obtain a Markovian transition matrix in the form of the following equations

$$[P] = \begin{bmatrix} 1 - \sum_{j=2}^n P_{1,j} & P_{1,2} & \dots & \dots & P_{1,n} \\ 0 & 1 - \sum_{j=3}^n P_{2,j} & \dots & \dots & P_{2,n} \\ \dots & \dots & \dots & \dots & \dots \\ 0 & \dots & 0 & 1 - P_{(n-1),n} & P_{(n-1),n} \\ 0 & \dots & \dots & 0 & 1 \end{bmatrix} \quad (9)$$

The matrix is structured to have rows and columns that correspond to damage levels placed in ascending order; the first level represents the structure as-new while the last one represents the collapse. the

failure level is defined as an absorbing state since once the condition has been reached it is not possible to go back, as consequence the transition matrix is triangular higher because of the monotonic nature of the deterioration.

The following image describe the discretization of degradation states of a damage-accumulating structure:

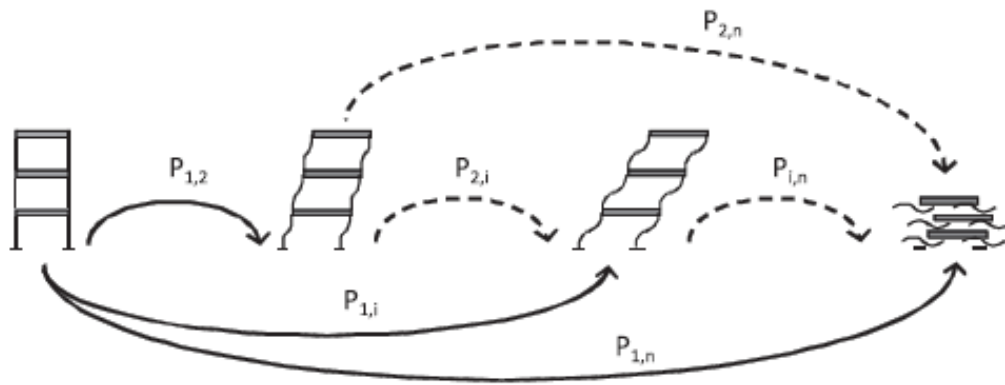


Figure 3.2. scheme of degradation states of a damage-accumulating structure.

If the frequency unit-time event of earthquake shock is small enough to afford to neglect the probability of observing more than one earthquake in the range of unit time; for each pair of DS ($i \neq j$), the probability that the structure passes from one to another in a unit time interval ($k, k + 1$) can be calculated as the rate of earthquakes filtered by the probability that the structure move between the two states, given the presence of an event.

$$P[j - th \text{ state at } (k + 1) | i - th \text{ state at } k] = \nu_E \cdot P_{i,j} \quad (10)$$

The matrix reporting the probabilities of the structure moving between any two states in a unit-time interval, ($k, k+1$), is given by Equation.

$$\begin{aligned}
& [P_E(k, k + 1)] = v_E \cdot [P] + (1 - v_E) \cdot [I] \\
& = \begin{bmatrix} 1 - \sum_{j=2}^n v_E \cdot P_{1,j} & v_E \cdot P_{1,2} & \dots & \dots & v_E \cdot P_{1,n} \\ 0 & 1 - \sum_{j=2}^n v_E \cdot P_{2,j} & \dots & \dots & v_E \cdot P_{2,n} \\ \dots & \dots & \dots & \dots & \dots \\ 0 & \dots & 0 & 1 - v_E \cdot P_{(n-1),n} & v_E \cdot P_{(n-1),n} \\ 0 & \dots & \dots & 0 & 1 \end{bmatrix} \quad (11) \\
& = [P_E]
\end{aligned}$$

Through transition matrix we can completely define the damage accumulation process as an homogeneous Markovian chain. If we want to know the transition matrix from m time units: $[P_E(k, k+m)]$ we should raise to mth power the unit transition matrix previous seen, obtaining:

$$\begin{aligned}
& [P_E(k, k + m)] \\
& = \begin{bmatrix} 1 - \sum_{j=2}^n v_E \cdot P_{1,j} & v_E \cdot P_{1,2} & \dots & \dots & v_E \cdot P_{1,n} \\ 0 & 1 - \sum_{j=2}^n v_E \cdot P_{2,j} & \dots & \dots & v_E \cdot P_{2,n} \\ \dots & \dots & \dots & \dots & \dots \\ 0 & \dots & 0 & 1 - v_E \cdot P_{(n-1),n} & v_E \cdot P_{(n-1),n} \\ 0 & \dots & \dots & 0 & 1 \end{bmatrix}^m \quad (12) \\
& = [P_E]^m
\end{aligned}$$

The probability that the damage does not exceed a level d up to time n is

$$P[D < d|n] = \sum_{i=1}^n p_{ij}^m = Q^m \quad (13)$$

Where $Q^m = p_{ij}^m$ is the m-th product of $Q = (p_{ij}, I, j < d)$.

To evaluate the probability of finding the structure in any of the possible states at time $k+m$ in any of the possible states given a vector (size $1 \times n$) collecting the (initial) probabilities of structure being in one of the states at k $[P_1^0 P_2^0 \dots P_n^0]$ we have to multiply this vector for the previous one:

$$[P_1^0 P_2^0 \dots P_n^0] \cdot Q^m \quad (14)$$

Thus, the exceedance probability is equal to:

$$P[D > d|n] = 1 - [P_1^0 P_2^0 \dots P_n^0] \cdot Q^m \quad (15)$$

3.4 Frequentist probability

The theoretical probability of an event is the ratio between the number of favourable cases and the number of supposed possible cases all equally possible

$$P[D > d|n] = \frac{\sum N(D>d)}{N_{tot}} \quad (16)$$

Where $N(D > d)$ is the number of samples that exceed a given level d while N_{tot} is the number of total samples used for the analysis.

4 STRUCTURAL MODELS

4.1 Introduction

Performance-based earthquake engineering (PBEE) addresses the economic impact on structural damage for a given level of danger. Therefore, it is necessary to devise models to predict the damage corresponding to a given earthquake. This has led to the emergence of modern modelling techniques such as the fibre-based finite element technique, the most advantageous method for non-linear analysis of frame structures.

This technique involves in dividing the cross-section of the element into a number of fibres placed at certain points of the element called "integration points".

Each fibre is assigned a uniaxial non-linear material model that allows to describe its behaviour. Every material that makes up the section as reinforcing steel, confined and unconfined concrete is treated as separate material models at the section level. Therefore, the response of the component is mainly controlled by the inelastic response of the cross section.

4.2 Finite element model of RC bridge columns

Two bridge piers of different heights are employed in this study. These columns are taken from the experimental test units reported in (Lehman DE, 2000). The same ID as used in the experiment is employed here to identify these columns. In t (Kashani M. , 2017) the following Table are summarised the details of the selected columns and their references, in this table is possible to find information about the column length L , the L/D ratio is column length to column diameter ratio, ρ_l is the ratio of longitudinal reinforcement area to total cross sectional area, ρ_h is the

volumetric ratio of horizontal reinforcement and $P/(A_g f_c)$ is the axial force ratio, where P is the axial force on the column, A_g is the gross cross section area of column and f_c is the compressive strength of concrete.

Table 3. Details of column dataset

ID	Reference	L(mm)	L/D	ρ_l (%)	ρ_h (%)	$P/(A_g f_c)$
3	Lehman and Moehle 815	4876.8	8	1.49	0.01	0.07
4	Lehman and Moehle 1015	6096	10	1.49	0.01	0.07

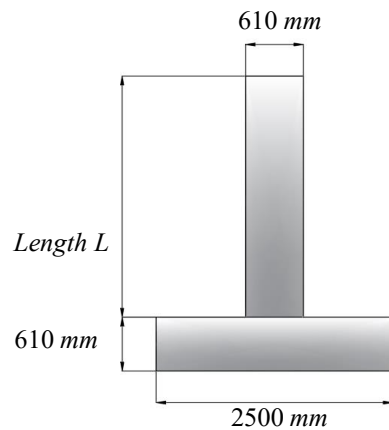


Figure 4.1 Schematic view of the experimental units tested by Lehman and Moehle (2000)

In order to formulate distributed plasticity frame models Kashani uses a force-based formulation in which the internal force fields are expressed as functions of the nodal forces. A fibre beam-column element is a line element in which the moment–curvature response at selected locations (along the element known as integration points) is determined from the fibre section assigned to that integration point.

The choice of a force-based element is due to its adaptability to non-linear analysis because they grant the diffusion of plasticity over the length of the member using one element that has multiple integration

points. These elements have a limit, they can lose their objectivity at a locally or globally depending on section hardening or softening behaviour. This implies that the buckling will occur at the first critical section of the column, so we choose the integration length of this section equal to the buckling length. In the present work two force-based elements are used to model the RC columns. For the first element with total length of $6 L_{eff}$, where L_{eff} is the buckling length, are used three integration points (using Gauss–Lobatto integration scheme).

Using this method, the length of the first element at the bottom of the column is adjusted based on the buckling length for each column.

The second element, aimed to model the top part of the column, presents five integration points. The strain penetration and the slippage of reinforcement anchored to the foundation are modelled through a zero-length section element available in the OpenSees. Below is shown a schematisation of the used model.

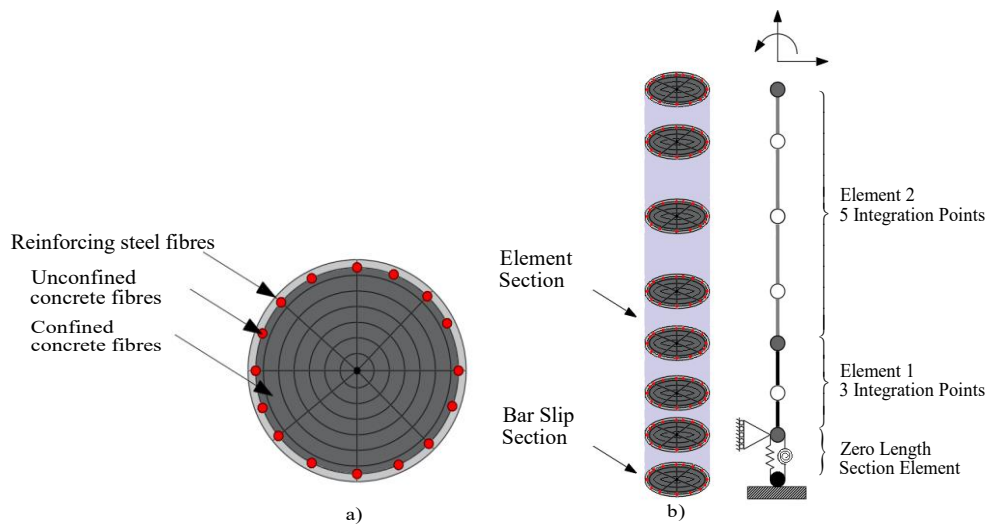


Figure 4.2 Schematization of a fibre beam-column element with bar buckling and bar slip model.

4.3 Materials

In the last decades the non-linear analysis of reinforced concrete structures has taken hold, this has led to the development of the fibre element technique. In this approach the member cross section is decomposed into several steel and concrete fibres at selected integration points. The material nonlinearity is represented through a uniaxial constitutive material model of steel, in tension and compression, and concrete, confined core concrete and unconfined cover concrete. In the following pages the uniaxial materials employed for the structural model will be illustrated.

4.3.1 Confined and unconfined concrete model

To model concrete behaviour the uniaxial material Concrete04 available in OpenSees is used; it is employed to model the unconfined concrete behaviour in cover concrete and a in confined concrete. For loading in compression, the envelope to the stress-strain curve follows the model proposed by Popovics (Popovics, 1988;) until the concrete crushing strength is achieved and for strains beyond that corresponding to the crushing strength. The confined concrete is modelled using the confinement parameters developed by Mander et al. (Mander JB, 1988) Fig.4.3 (a) shows the confined and unconfined concrete models with unloading–reloading cycling rules. Fig.4.3 (b) shows the concrete model in tension with unloading–reloading cycling rules.

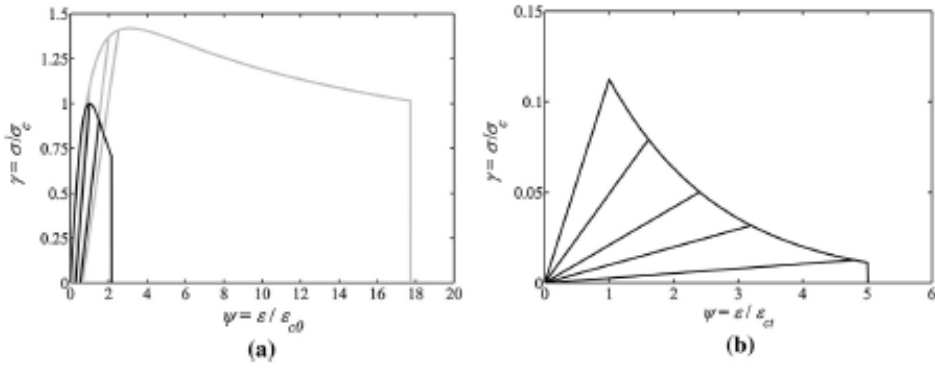


Figure 4.3 Cyclic response of concrete model employed in the analyses: (a) unconfined and confined concrete response in compression including cyclic response; (b) tension.

4.3.2 Reinforcing steel model

The uniaxial Hysteretic material model in the OpenSees is the generic hysteric model is used to model stress–strain behaviour of a material or force–displacement behaviour of steel reinforcement. Buckling of vertical reinforcing bars is one of the most common observed collapse mechanisms of RC structures in the past earthquakes which ultimately results in crushing of core concrete in RC columns.

Therefore, in the recent years several researchers have put efforts to develop analytical models to capture the buckling behaviour of vertical reinforcing bars within the RC elements. In this research the Dhakal and Maekawa analytical model is used to explain the post-yield buckling behaviour of reinforcing bars, taking into account the interaction of the vertical reinforcement and horizontal tie reinforcement. In this model, the post-yield buckling response of reinforcement is defined as a function of a compound variable called the nondimensional slenderness ratio λ_p as defined in the following equation:

$$\lambda_p = \sqrt{\frac{\sigma_y}{100}} \frac{L}{D} \quad (17)$$

where σ_y is the yield strength of reinforcement in MPa.

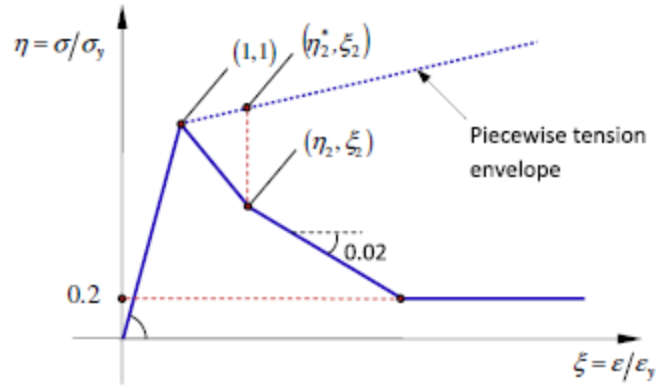


Figure 4.4 Dhakal and Maekawa buckling model.

The stress–strain envelope shown in the previous figure is described by the following equations:

$$\eta = \begin{cases} \xi; & \xi \leq 1 \\ \frac{(\eta_2-1)}{(\xi_2-1)} (\xi - 1) + 1 & 1 \leq \xi \leq \xi_2 \\ \eta_2 - 0.02, (\xi - \xi_2) & \xi_2 \leq \xi, \eta \geq 0.2 \\ 0.2 & \text{otherwise} \end{cases} \quad (18)$$

where, the empirical relationships for (ξ_2, η_2) are given below:

$$\xi_2 = 55 - 2.3\lambda_p; \quad \xi_2 \geq 7 \quad (19)$$

$$\eta_2 = \alpha(1.1 - 0.016\lambda_p)\eta_2^* \quad \eta_2 \geq 0.2 \quad (20)$$

Where η_2^* is the non-dimensional piecewise stress corresponding to the η_2 . The value of α is a softening coefficient and depends on the strain hardening of reinforcement assumed equal to 0.75.

4.3.3 Low-cycle fatigue degradation model

To account for the effect of low-cycle fatigue it has been used a uniaxial Fatigue material model available in OpenSees. It can be wrapped to any steel model without changing the stress–strain state of the parent material. The model employs a modified rain-flow cycle counter to track strain amplitudes. The cycle counter is used in conjunction with Coffin–

Manson relationship and Miner's Rule to describe the low-cycle fatigue failure:

$$\varepsilon_p = \varepsilon_f (2N_f)^{-\alpha} \quad (21)$$

where ε_p is the plastic strain amplitude ($\varepsilon_p = \varepsilon_a - \varepsilon_e$ where, ε_a is the total strain amplitude and ε_e is the elastic strain), $2N_f$ is the number of half-cycles to failure and α and ε_f are material constants. By wrapping this model to any steel model, once the Fatigue material reaches a damage state of 1.0, the stress of the parent material becomes zero. An example graph of the Fatigue material model wrapped to Steel02 is shown in Fig. 4.6.

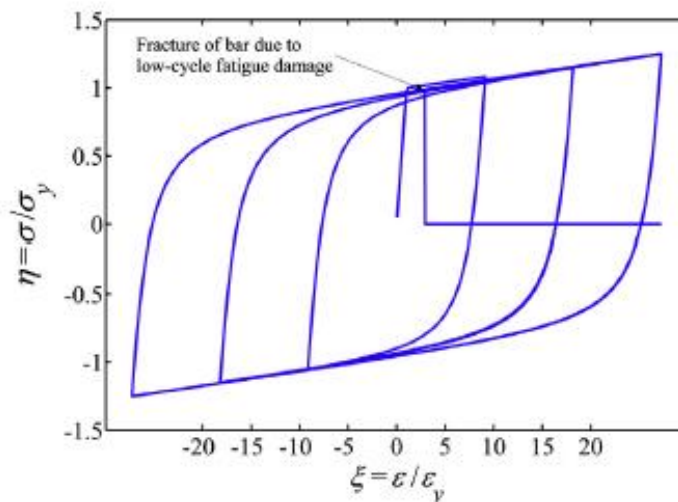


Figure 4.5 Fatigue material model to predicting the fracture of reinforcement due to low-cycle fatigue

4.3.4 Bond-slip displacement model for zero length element

4.3.4.1 Tensile stress-slip model for reinforcing steel

In seismic design of RC bridge piers, plastic hinges are designed to form at the column ends (column to foundation/capping beam connection). This will result in slippage of longitudinal bars due to the substantial strain penetration along the bars into the foundation. (Kashani, 2016)

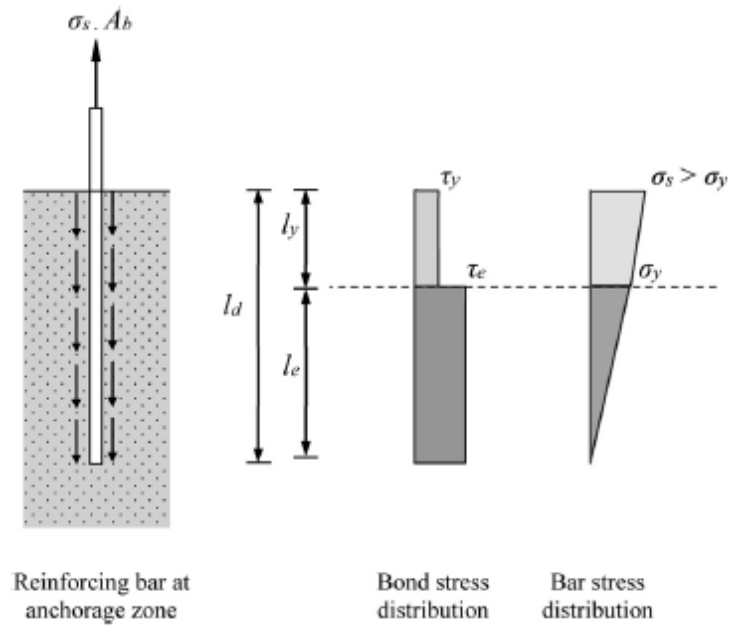


Figure 4.6 Bar slip model

Using the model in Fig. 4.7 the bar stress–slip relationship can be calculated using the Eqs:

$$slip = \int_0^{l_{\sigma_s}} \tau_e \frac{\pi d_b}{A_b} \frac{1}{x} dx \Rightarrow slip = \frac{2\tau_e l_{\sigma_s}^2}{E d_b} \quad \forall \sigma_s < \sigma_y \quad (22)$$

$$slip = \int_0^{l_e} \frac{4\tau_e}{d_b} \frac{1}{E} x dx + \int_{l_e}^{l_e+l_y} \left(\frac{\sigma_y}{E} + \tau_y \frac{4(x-l_e)}{d_b E} \right) dx \quad (23)$$

$$\Rightarrow slip = \frac{2\tau_e l_e^2}{E d_b} + \frac{\sigma_y l_y}{E} + \frac{\tau_y l_y^2}{E_h d_b} \quad (24)$$

$$l_{\sigma_s} = \frac{\sigma_s}{\tau_e} \cdot \frac{A_b}{\pi d_b} \quad (25)$$

$$l_e = \frac{\sigma_y}{\tau_e} \cdot \frac{A_b}{\pi d_b} \quad (26)$$

$$l_y = \frac{\sigma_s - \sigma_y}{\tau_y} \cdot \frac{A_b}{\pi d_b} \quad (27)$$

where σ_s is bar stress at the column–foundation perimeter; σ_y is yield strength of reinforcing bar; E is steel elastic modulus; E_h is steel hardening modulus assuming a bilinear stress–strain response; τ_e is bond strength for elastic steel; τ_y is bond strength for yielded steel; A_b is

nominal bar cross section area; and d_b is nominal bar diameter and l_e and l_y , are the lengths along the reinforcing bar for which steel stress is less than and greater than the yield stress respectively.

The suggested value of steel hardening ratio (E_h/E) is suggested to be taken as 0.1. The stress–slip model of confined concrete model used in zero length section is shown in Fig. 4.7.

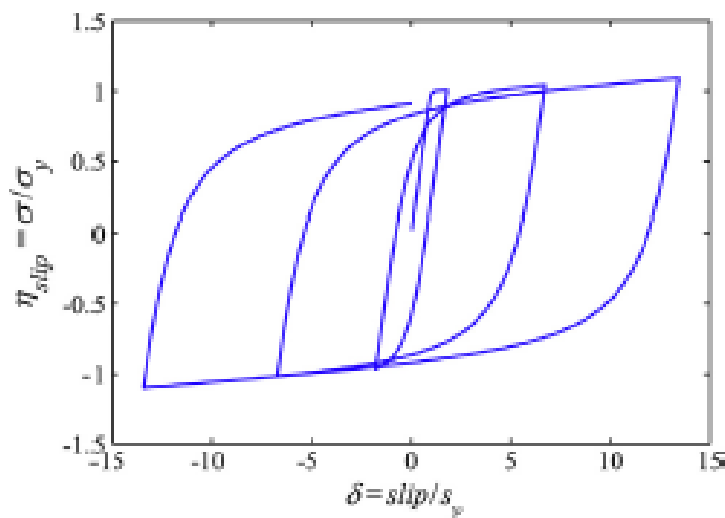


Figure 4.7 Bar stress–slip model used in zero length section.

4.3.4.2 Compressive stress–slip model for concrete

The slippage of longitudinal bars in tension combined with the compression due to flexure and axial force results in a highly localised compressive stress in concrete in compression zone. This will cause a localised damage in confined concrete over a so-called d_{comp} depth as shown in Fig. 4.8.

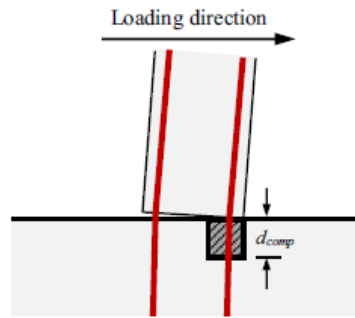


Figure 4.8 Assumed compressive depth

The recommended value of d_{comp} to be $0.5c$ where c is the depth of neutral axis. In this study $d_{comp} = 0.3D$ is used in the analyses where D is the column diameter. The uniaxial material Concrete01 available in the OpenSees (concrete model with zero tension) is used to model the concrete in zero length section. The stress–strain behaviour of this model is modified by multiplying the strain by d_{comp} . It should be noted that the whole zero length section was considered for confined concrete. The stress–slip model of confined concrete model used in zero length section is shown in Fig. 4.9.

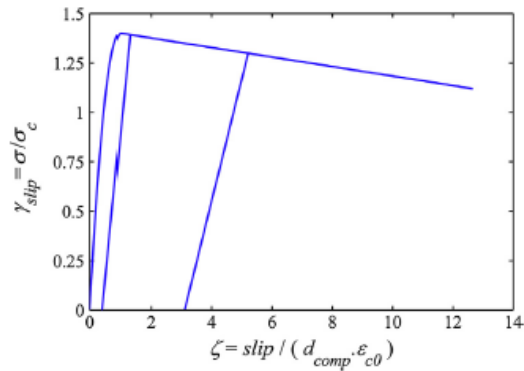


Figure 4.9 Stress-slip model

5 ILLUSTRATIVE APPLICATIONS OF THE THREE METHODS TO THE MODELS

5.1 Introduction

During the internship at the university of Strathclyde in Glasgow the foundations of this work were laid. In order to evaluate different coupling between the dynamic system and the properties seismic input frequency content, the two columns with different characteristic periods, previously introduced, are considered to assess the seismic response. Specifically, the first phase involved the study of the models implemented with the finite element program OpenSees. Then, the abovementioned ones have been subjected to multiple earthquakes, with a number of occurrences pre-arranged, randomly extracted through Montecarlo simulation. In this approach, many earthquake intensity measures are sampled (300,1000,2500,3000) based on earthquake occurrence probabilities corresponding to site-specific seismic hazard curves. A dynamic analysis was carried out with which it was possible to evaluate stress, strain and displacements of interest, essential for the damage assessment. In the following paragraphs the results obtained from the application of the methodologies explained in chapter 3 are shown.

5.2 Ground motion selection

The uncertainties in the seismic input, record-to-record variability, are described by a statistical model. Generally, we can adopt two approaches for the probabilistic representation of ground motion. The first one, required the selection of a set of real ground motion records to represent the variability effects conditional to an IM value, whereas the second one, used for this work, is based on a fully stochastic representation of the seismic input. (Tubaldi, 2017) The most used stochastic ground motion models are the Atkinson and Silva (AS) ground motion (GM) model; in which the IM is described by defining a seismic source characterized by the moment magnitude M_m , the hypo-central distance R and the specification of a stochastic ground motion model accounting for the properties of the construction site. In the following table are reported the input data for our structures:

Table 4 Input data for ground motion generation.

ID	R_{mean} [Km]	M_{max}	M_{min}	T [s]	v_{eq}
815	10	8	5.5	0.69	0.0997
1015	10	8	5.5	0.94	0.0997

Where R_{mean} is the average hypo-central distance M_{max} and M_{min} are the maximum and minimum magnitude T is the period of the considered structure and v_{eq} is the mean annual frequency of earthquake of any magnitude.

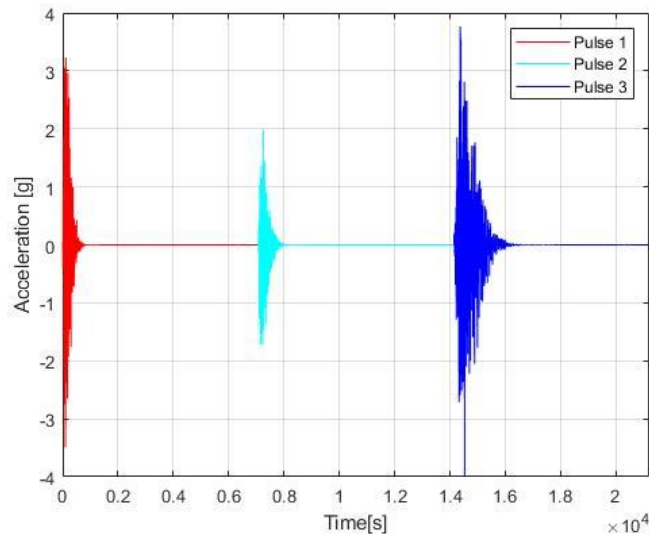


Figure 5.1 Representation of multiple earthquake.

Through GMAS method we have generated 5000 accelerograms. Then, with the Montecarlo method we have randomly extracted Intensity measures (IM) among those previously generated. The result is an increasing number (200, 300, 1000, 2500, 3500) of multiple earthquakes constituted by 20 occurrences that represent the seismic events that can occur in the life time of the structure that we have applied to the piers.

5.3 Results of Lehman and Mohel column 815

5.3.1 Ghosh et a. model

The work started for Ghosh et al. approach that focuses on the assessment of damage accumulation under repeated shocks while accounting for the probabilistic nature of the hazard. After choosing EDPs, regression models are developed. A preliminary investigation is carried out with increasing number of samples in order to find the number of samples that maximize the prestation of the regression model. Once defined this value, through a convergence study, to arrive at accurate estimates of damage index exceedance probabilities this study employs 50,000 Monte Carlo trials. Below you can find the results of applying this method for each EDPs.

5.3.1.1 Park and Ang damage index

The Park and Ang index for damage measurement results from a combination of ductility demand induced by the earthquake and the dissipated hysteretic energy.

$$D = \frac{u_{max}}{u_u} + \beta \frac{E_h}{F_y u_u}$$

Pertinent structural characteristics required for the damage index estimation, are presented in Table 4:

Table 5 Structural characteristic for column 815

Characteristic	Value
u_u [m]	0.6
u_y [m]	0.024
F_y [kN]	125
β	0.05

The fitted multilinear regression models now follow the form shown in Equation 5-6, conditioned on the PGA intensity of the latest pulse and

the damage incurred up to the previous shock. The images below show the results of linear and multilinear regression with the respective regression coefficients, with a number of sampled earthquakes increasing from 300 to 3500.

LINEAR REGRESSION

Looking at the figures it is possible to see that, despite the results from the analyses are very dispersed, the regression is quite good as shown by the value of the standard deviation of residuals (root mean square error) which leans towards zero.

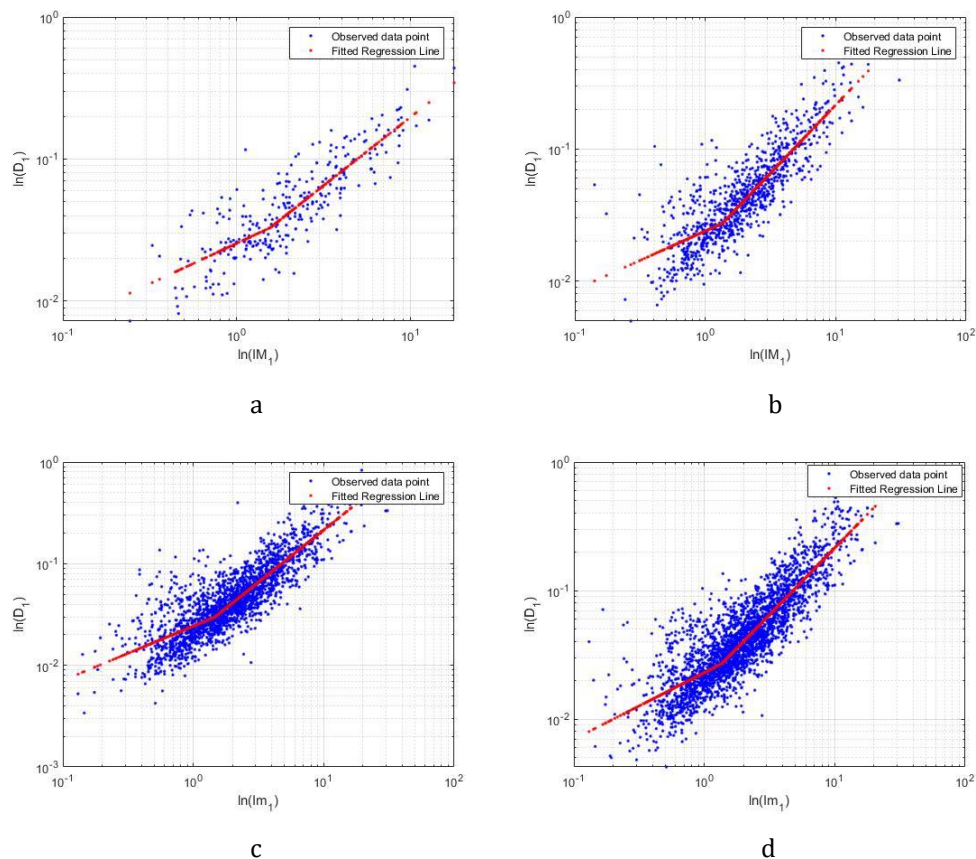


Figure 5.2 Linear regression model for predicting the damage index following single shock. Regression is carried out with an increasing number of samples a)300 b)1000 c)2500 d)3500

In the footer table the values of the regression coefficients are summarized with the respective errors. It should be noted that the increase in samples used for the regression does not significantly affect the results that remain almost unchanged.

Table 6 Regression coefficient and respective RMSE

Samples	α	β	γ	Sa*[m/s²]	ϵ_1	ϵ_2
300	-4.59	-0.48	0.9	1.55	0.61	0.37
1000	-3.73	0.45	1.03	1.35	0.47	0.35
2500	-3.71	0.53	1.02	1.46	0.46	0.37
3500	-3.77	0.51	1.04	1.36	0.44	0.37

MULTILINEAR REGRESSION

The regression surface seems to approximate very well the course of damage resulting from the analysis. It can be seen how increasing the number of samples significantly does not significantly improve the quality of the regression therefore, we will try to find the minimum number of samples that guarantees acceptable results.

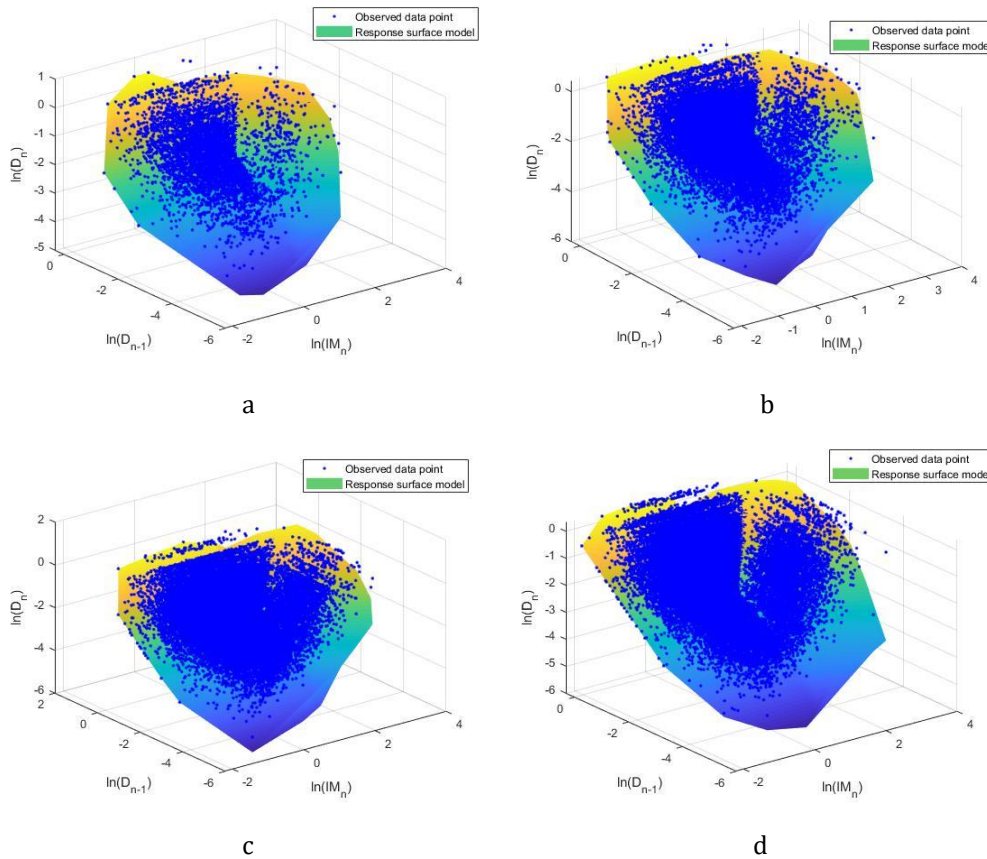


Figure 5.3 multilinear regression model for predicting the damage index after n shocks as a function of the PGA of the n th shock and the damage index of the previous one. Regression is carried out with an increasing number of samples a)300 b)1000 c)2500 d)3500

Even in this case, increasing the number of samples, no significant improvements were found.

Table 7 Regression coefficient and respective RMSE.

Samples	α	β	γ	δ	Sa*[m/s²]	ϵ_1	ϵ_2
300	-0.79	0.54	0.52	0	3.37	0.16	0.32
1000	-0.73	0.58	0.52	0	3.34	0.15	0.31
2500	-0.71	0.58	0.51	0	3.34	0.15	0.31
3500	-0.61	0.69	0.37	0	2.1	0.11	0.28

COMPUTATION OF DAMAGE INDEX EXCEEDANCE PROBABILITIES

Applying the procedure described in paragraphs 3.2.2, the following curves are obtained:

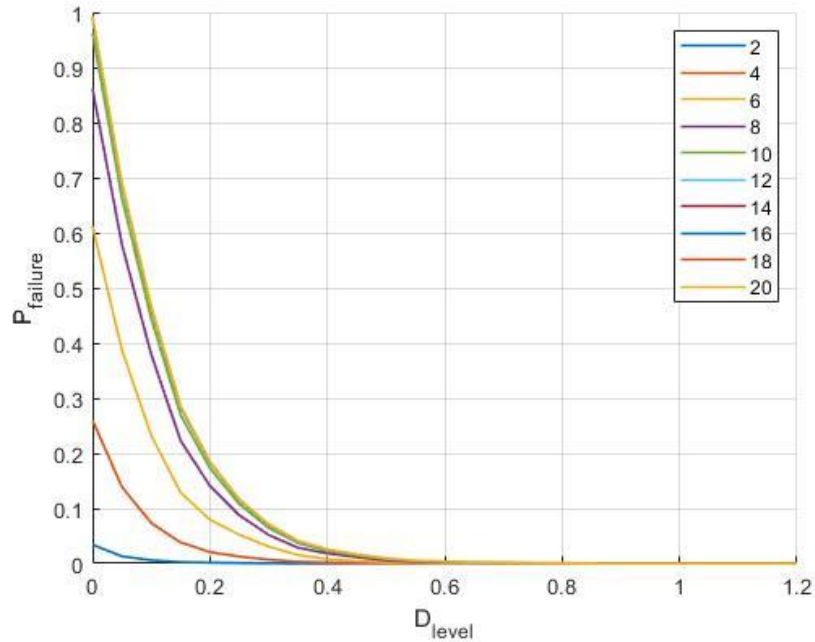


Figure 5.4 Probability of failure with an increasing number of occurrences.

They represent the probability of collapse for an increasing number of occurrences. Increasing the number of occurrences, the probability of collapse rises considerably reaching, after about ten earthquakes, the 100% of probability to overcome the first level of damage. We can see that to push the analysis beyond ten occurrences is useless since the curves for a number of earthquakes major than ten coincide.

CONVERGENCE STUDY

In order to optimize the treatment of Ghosh et al. by minimizing the number of samples to be analysed, a convergence study was performed. The procedures described above were performed with an increasing number of randomly extracted samples. The aim was to understand the number of samples beyond which it was not useful to push the analyses. The results of this study are visible in the figure 5.4.

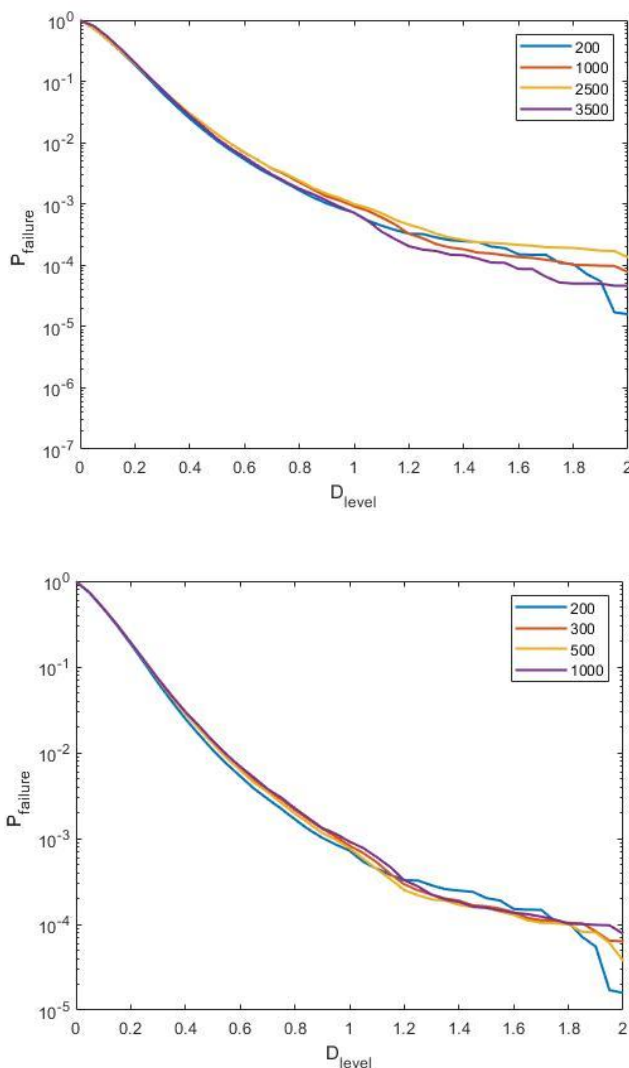


Figure 5.5 Probability of failure evaluated with an increasing number of samples

In the first instance the following cases were studied: 200, 1000, 2500 and 3500 samples. It was then realized that over 1000 the solutions coincided so it was useless to go beyond this value. Therefore, we sought values in the range between 200 and 1000 that would allow the analysis to be lightened without affecting its quality. The study was conducted for 300 and 500 samples, leading to the conclusion that by choosing a population of 300 samples we can optimize the results.

5.3.1.2 Maximum strain of confined concrete under compression

The confined concrete is modelled using the confinement parameters developed by Mander et al. The following figure shows the confined and unconfined concrete models with unloading-reloading cycling rules.

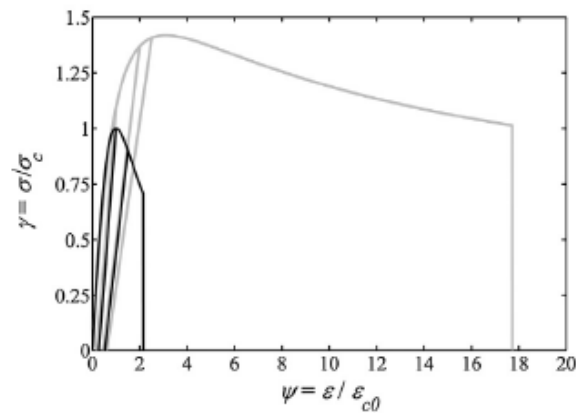


Figure 5.6 Cyclic response of confined concrete model under compression, employed in the analyses

Concrete failure may occur due to exceeding the maximum compressive strength and/or exceeding the maximum relative strain. In this case the maximum admissible deformation is 0.035.

LINEAR REGRESSION

Also in this case, even if the results from the analyses are very dispersed, the regression is quite good as shown by the value of the standard deviation of residuals (root mean square error) which leans towards zero. It is important to note the presence of a first horizontal section in the regression. This initially might seem an anomaly as the deformation of the concrete should have a monotonous increasing trend. However, this trend becomes logical if we consider that until a certain acceleration is reached, the axial forces prevail, which being constant do not lead to a deformation increase.

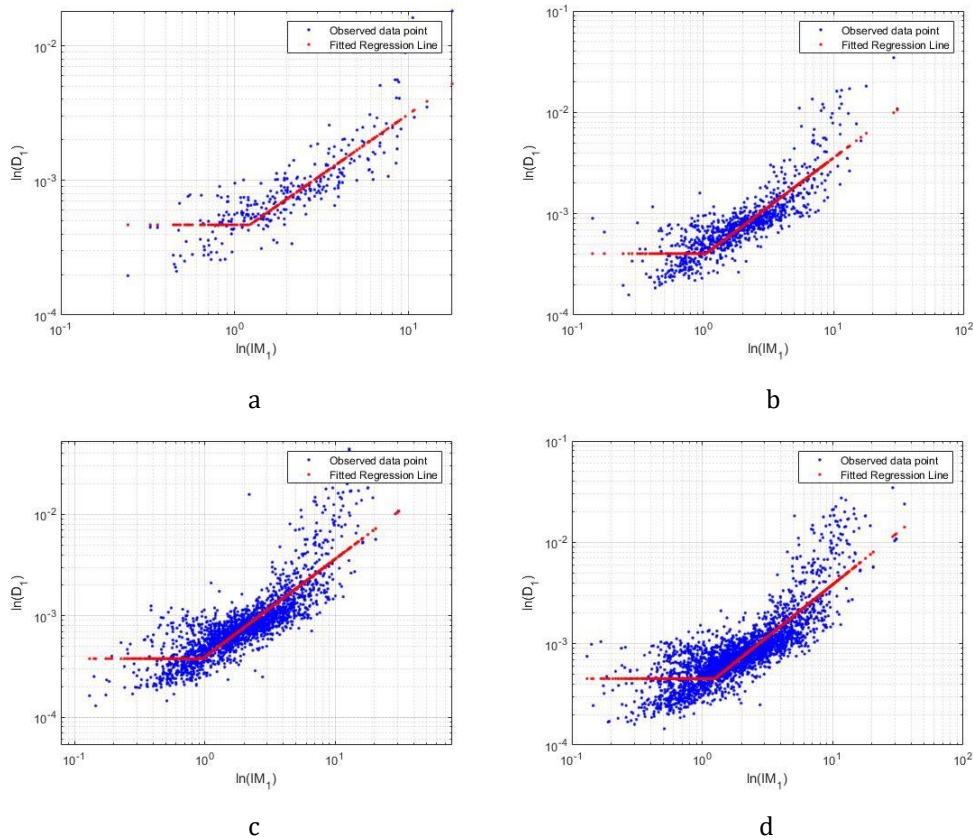


Figure 5.7 Linear regression model for predicting the damage index following single shock. Regression is carried out with an increasing number of samples a)300 b)1000 c)2500 d)3500

The following table contains the regression with the respective errors. We can notice that the increasing the number of samples used for the

regression does not significantly improve the results that remain almost unchanged.

Table 8 Regression coefficient and respective RMSE

Samples	α	β	γ	Sa*[m/s²]	ϵ_1	ϵ_2
300	-7.67	0.90	0.19	1	0.39	0.34
1000	-7.81	0.96	0.05	1	0.39	0.37
2500	-7.884	0.967	-0.038	1	0.4	0.41
3500	-7.7	1.02	0.22	1	0.44	0.41

MULTILINEAR REGRESSION

Although the visible data dispersion, the regression model shows good accuracy. Increasing largely the number of samples does not significantly improve the quality of the regression therefore, we will try to find the minimum number of samples that guarantees acceptable results.

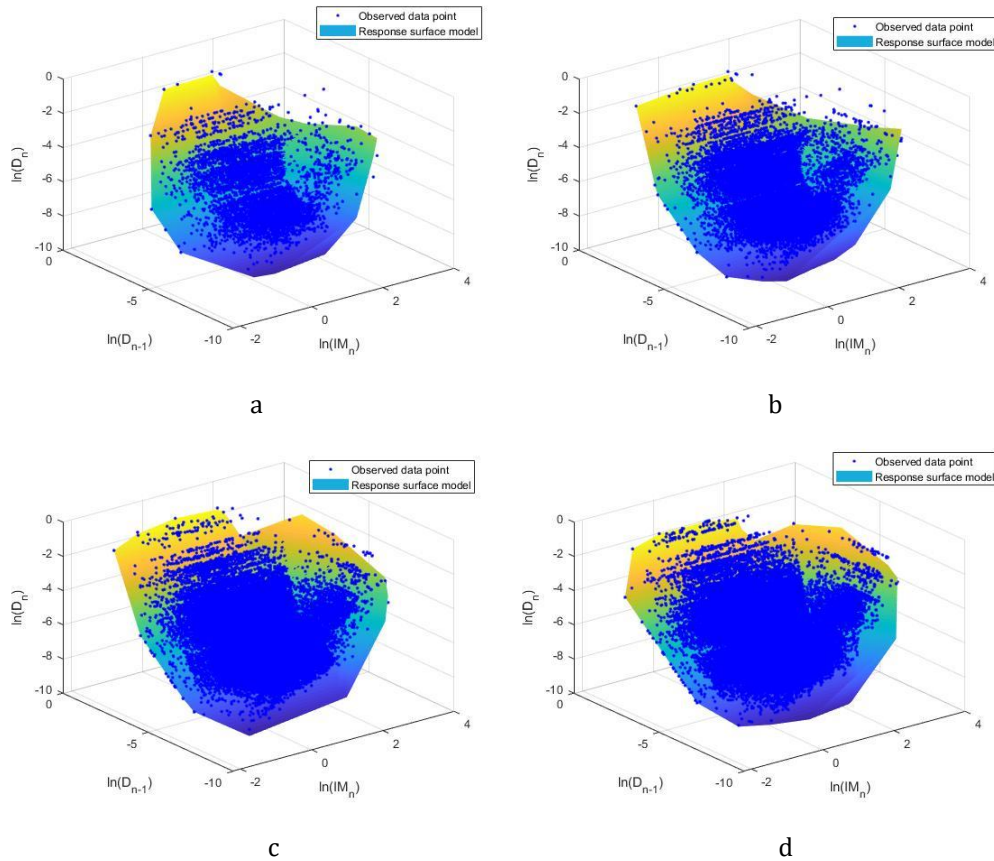


Figure 5.8 multilinear regression model for predicting the damage index after n shocks as a function of the PGA of the n th shock and the damage index of the previous one. Regression is carried out with an increasing number of samples a)300 b)1000 c)2500 d)3500

Table 9 Regression coefficients and respective RMSE.

Samples	α	β	γ	δ	$Sa^*[\text{m/s}^2]$	ϵ_1	ϵ_2
300	-0.64	0.88	-1.75	-0.49	4.15	0.14	0.54
1000	-0.65	0.88	-1.88	-0.51	4.02	0.14	0.5
2500	-2.40	0.54	1.37	0	6.1	0.2	0.60
3500	-2.53	0.52	1.39	0	6.09	0.19	0.63

COMPUTATION OF EDPs EXCEEDANCE PROBABILITIES

The procedure described in paragraphs 3.2.2, lead to the following results:

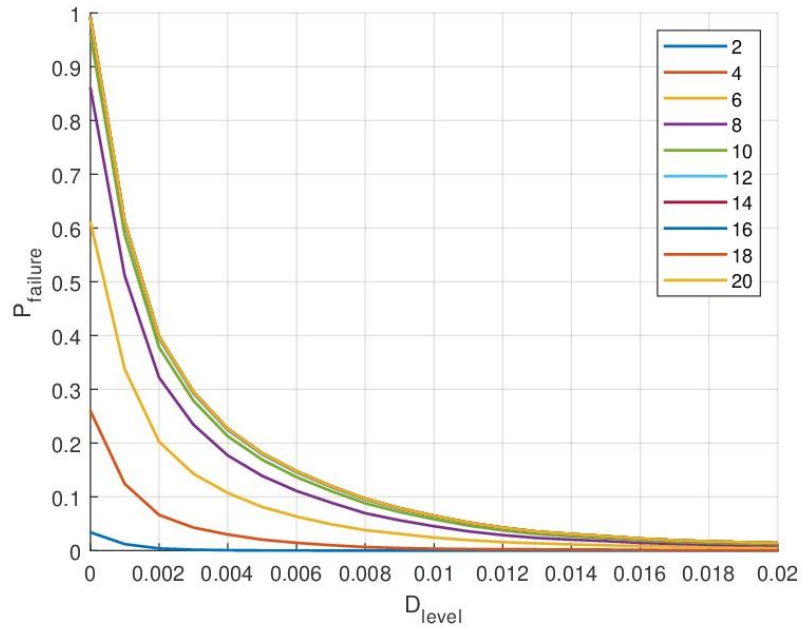


Figure 5.9 Probability of failure with an increasing number of occurrences.

This figure shows how the increase in the number of earthquakes that can occur in the life of the structure increases the probability of collapse. After about ten earthquakes the 100% of probability to overcome the first level of damage is reached. We can see that to push the analysis beyond ten occurrences is useless since the curves for a number of earthquakes major than ten coincide.

CONVERGENCE STUDY

Also in this case a convergence study was performed in order to optimize Ghosh et al. method, by minimizing the number of samples to be analysed. We perform the procedures described in chapter 3 with an increasing number of randomly extracted samples. The aim was to understand the number of samples beyond which it was not useful to push the analyses. The results of this study are visible in the Figure 5.9.

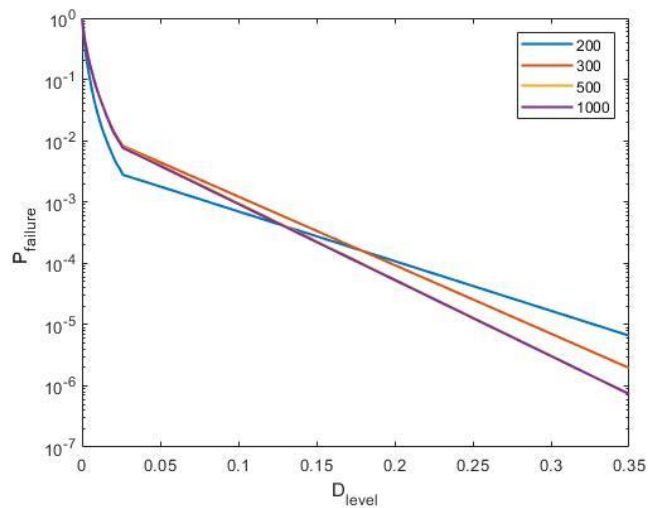
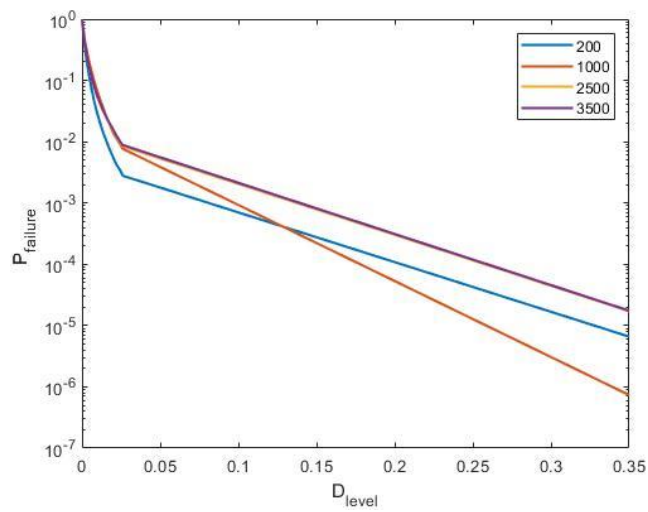


Figure 5.10 Probability of failure evaluated with an increasing number of samples.

5.3.1.3 Maximum strain of unconfined concrete under compression

The unconfined concrete is modelled using the confinement parameters developed by Mander et al. The following figure shows the confined and unconfined concrete models with unloading–reloading cycling rules.

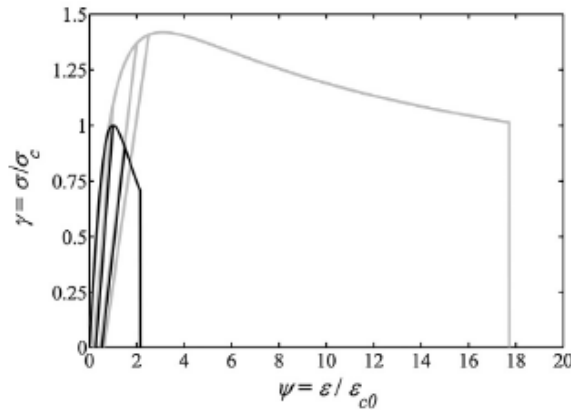
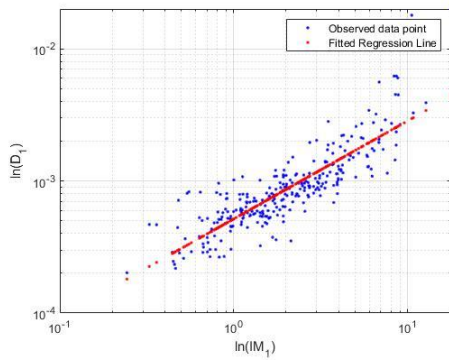


Figure 5.11 Cyclic response of unconfined concrete model under compression, employed in the analyses.

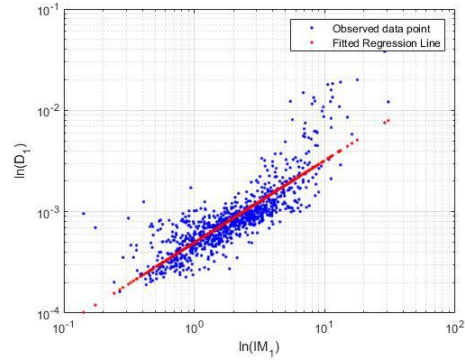
Concrete failure may occur due to exceeding the maximum compressive strength and/or exceeding the maximum relative strain. In this case the maximum admissible deformation is 0.00428.

LINEAR REGRESSION

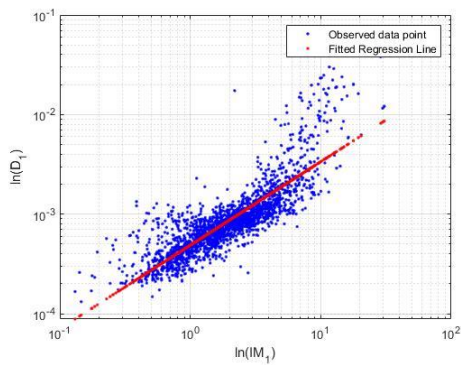
The regression carried out with an increasing number of samples returned the results shown in the figure 5.11. Looking at the figures it is possible to see that, despite the results from the analyses are very dispersed, the regression is quite good as shown by the value of the standard deviation of residuals (root mean square error) which leans towards zero.



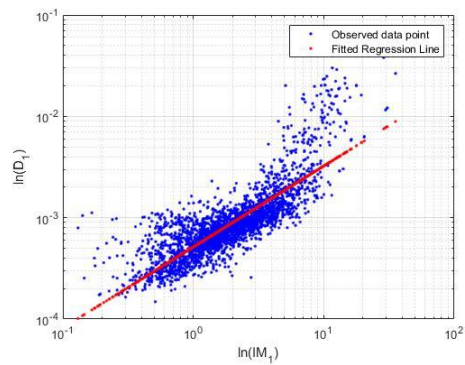
a



b



c



d

Figure 5.12 Linear regression model for predicting the damage index following single shock. Regression is carried out with an increasing number of samples a)300 b)1000 c)2500 d)3500

Table 10 Regression coefficients and respective RMSE.

Samples	α	β	γ	Sa*[m/s ²]	ϵ_1	ϵ_2
300	-7.56	0.74	1	1	0.38	0.35
1000	-7.81	0.97	0.05	1	0.39	0.37
2500	-7.63	0.84	1	1	0.45	0.43
3500	-7.57	0.79	1	1	0.50	0.44

MULTILINEAR REGRESSION

As can be seen from the images below, the regression produced good results. However, increasing the number of samples significantly does not significantly improve the quality of the regression therefore, we will try to find the minimum number of samples that guarantees acceptable results.

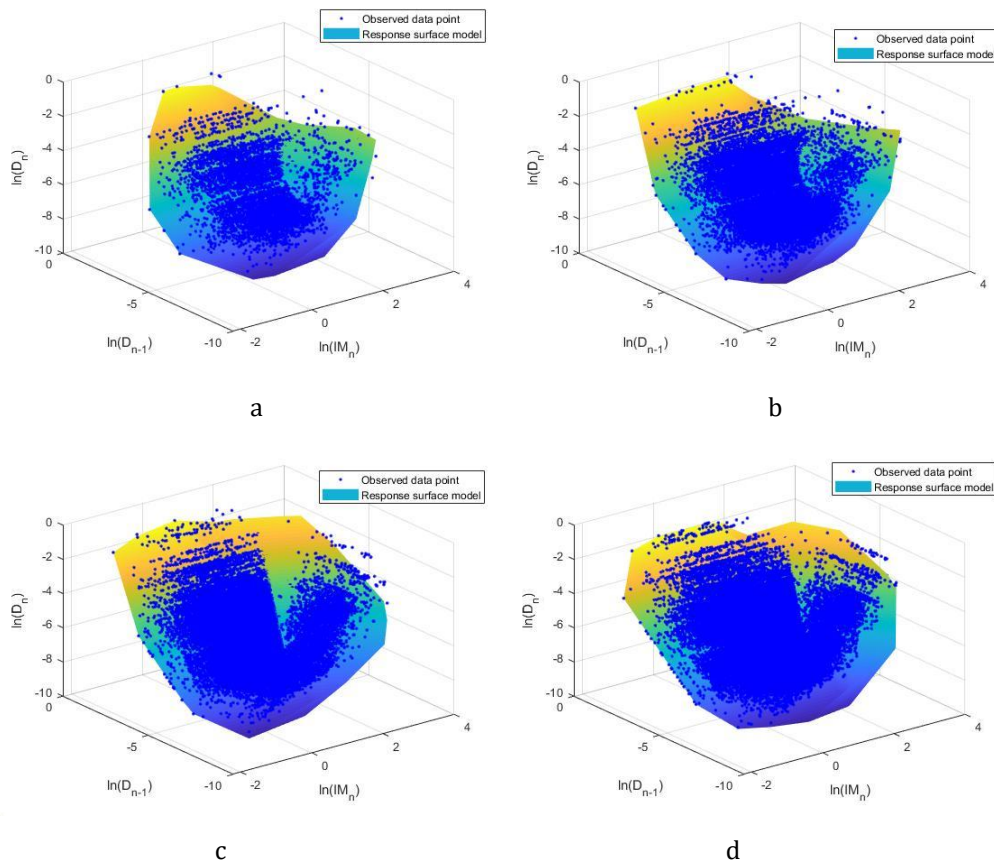


Table 11 Multilinear regression model for predicting the damage index after n shocks as a function of the PGA of the n th shock and the damage index of the previous one. Regression is carried out with an increasing number of samples a)300 b)1000 c)2500 d)3500

Table 12 Regression coefficients and respective RSME.

Samples	α	β	γ	δ	$Sa^*[m/s^2]$	ϵ_1	ϵ_2
300	-0.57	0.90	-1.70	0	3.9	0.14	0.51
1000	-0.65	0.88	-1.88	0	4.3	0.14	0.50
2500	-1.31	0.79	0.66	0	2.36	0.10	0.44
3500	-0.21	0.63	1.10	0	4.28	0.15	0.56

COMPUTATION OF EDPs EXCEEDANCE PROBABILITIES

Applying the procedure described in paragraphs 3.2.2, the following curves are obtained:

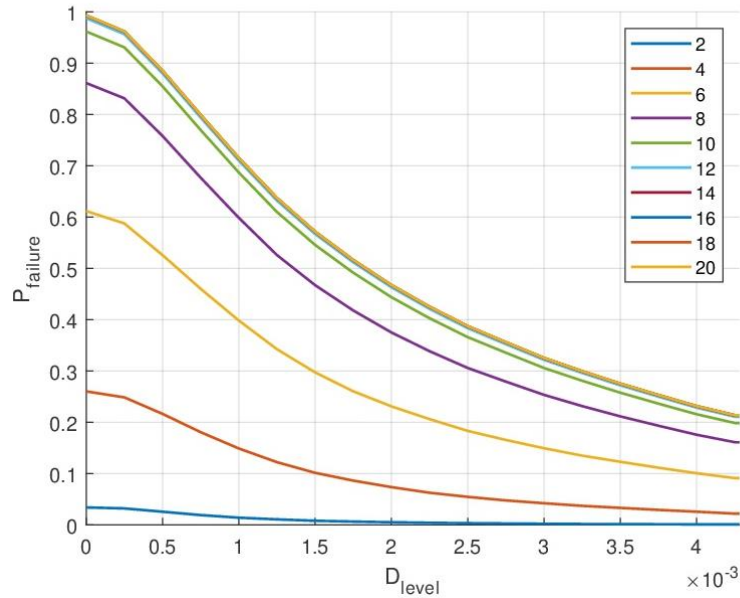


Figure 5.13 Probability of failure with an increasing number of occurrences.

As said before it is sufficient consider 10 occurrences in the design life of the structure, in this case equal to 50 years, because beyond this value the failure probability became insensitive with respect to the number of occurrences.

CONVERGENCE STUDY

In order to optimize the treatment of Ghosh et al. by minimizing the number of samples to be analysed, a convergence study was performed. The procedures described above were performed with an increasing number of randomly extracted samples. The aim was to understand the number of samples beyond which it was not useful to push the analyses. The results of this study are visible in the Fig. 5.13

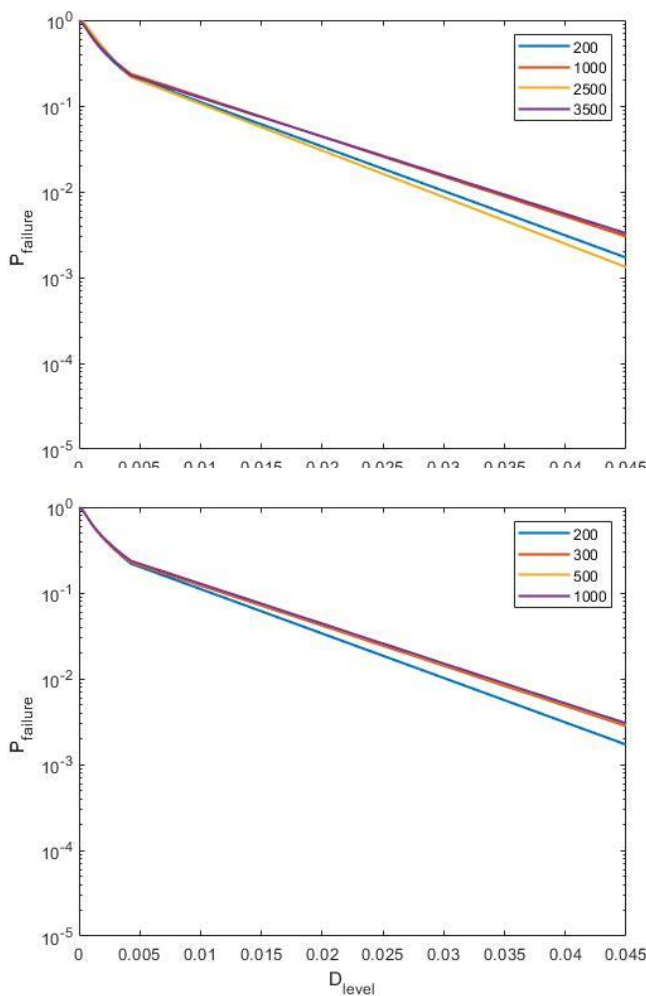


Figure 5.14 Probability of failure evaluated with an increasing number of samples.

In the first instance the following cases were studied: 200, 1000, 2500 and 3000 samples. It was then realized that over 1000 the solutions coincided so it was useless to go beyond this value. Therefore, we sought values in the range between 200 and 1000 that would allow the analysis to be lightened without affecting its quality.

The study was conducted for 300 and

500 samples, leading to the conclusion that by choosing a population of 300 samples we can optimize the results.

5.3.1.4 Maximum strain of unconfined concrete under tension

The unconfined concrete is modelled using the confinement parameters developed by Mander et al. The following figure shows the concrete model in tension with unloading–reloading cycling rules.

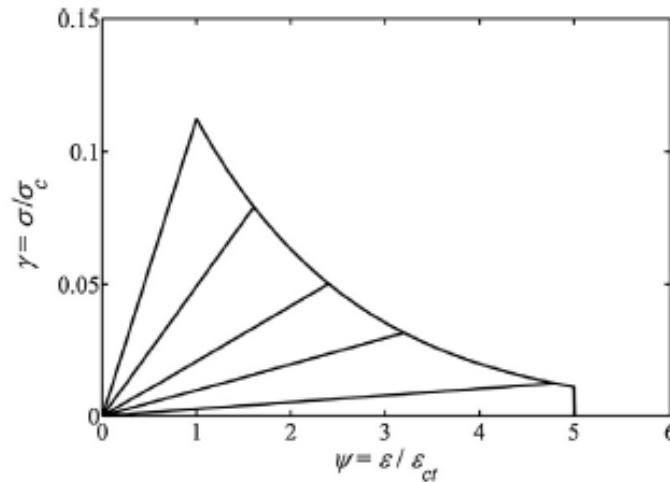


Figure 5.15 Cyclic response of unconfined concrete model under tension, employed in the analyses

Concrete failure may occur due to exceeding the maximum tensile strength and/or exceeding the maximum relative strain. In this case the maximum admissible deformation is 0.00125.

LINEAR REGRESSION

Looking at the figures it is possible to see that, despite the results from the analyses are very dispersed, the regression is quite good as shown by the value of the standard deviation of residuals (root mean square error) which leans towards zero. We have to underline the presence of a first horizontal trend in the regression. This initially, might seem an anomaly as the deformation of the concrete should have a monotonous increasing trend. However, this tendency becomes logical if we consider that until a certain acceleration is reached, the axial forces prevail, which being constant do not lead to a deformation increase.

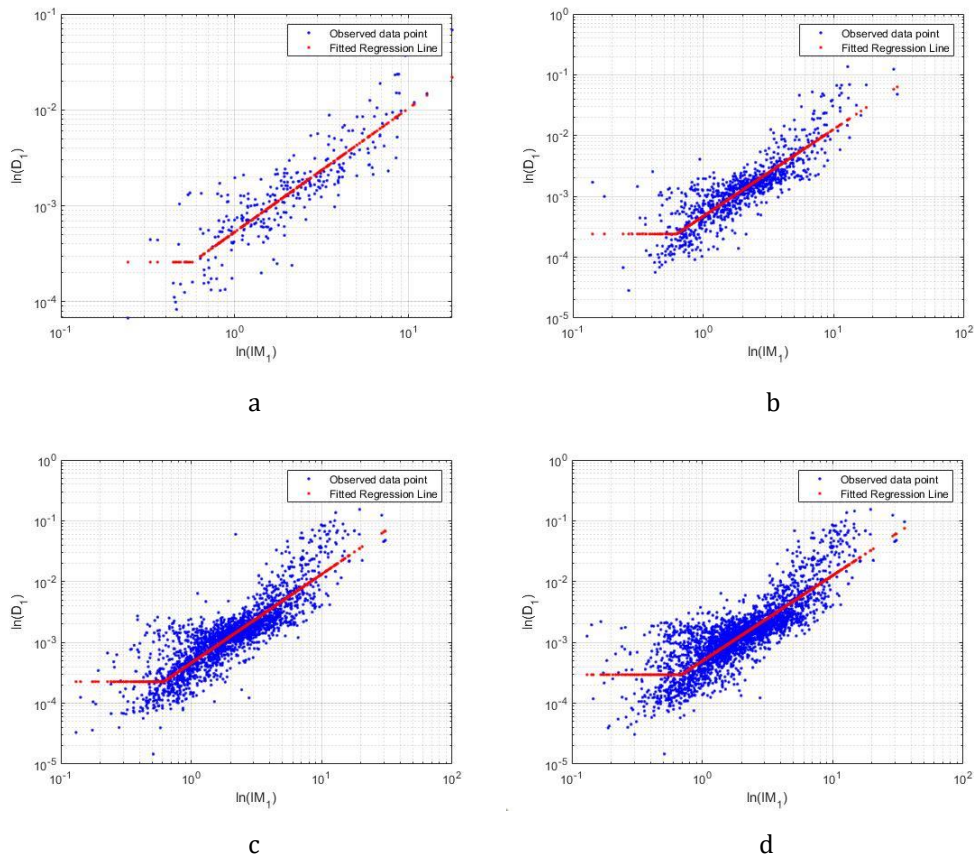


Figure 5.16 Linear regression model for predicting the damage index following single shock. Regression is carried out with an increasing number of samples a)300 b)1000 c)2500 d)3500

In the footer table the values of the regression coefficients are summarized with the respective errors.

Table 13 Regression coefficients and respective RMSE.

Samples	α	β	γ	$Sa^* [m/s^2]$	ϵ_1	ϵ_2
300	-8.26	1.29	-0.56	1	0.76	0.52
1000	-8.3	1.43	-0.46	1	0.8	0.55
2500	-8.39	1.46	-0.48	1	0.82	0.58
3500	-8.13	1.41	-0.36	1	0.89	0.59

MULTILINEAR REGRESSION

The results of linear regression are shown below, as we can see there is quite high dispersion, however, regression model is able to catch the trend. The following figures show the result of the application of predictive equations in chapter 3.

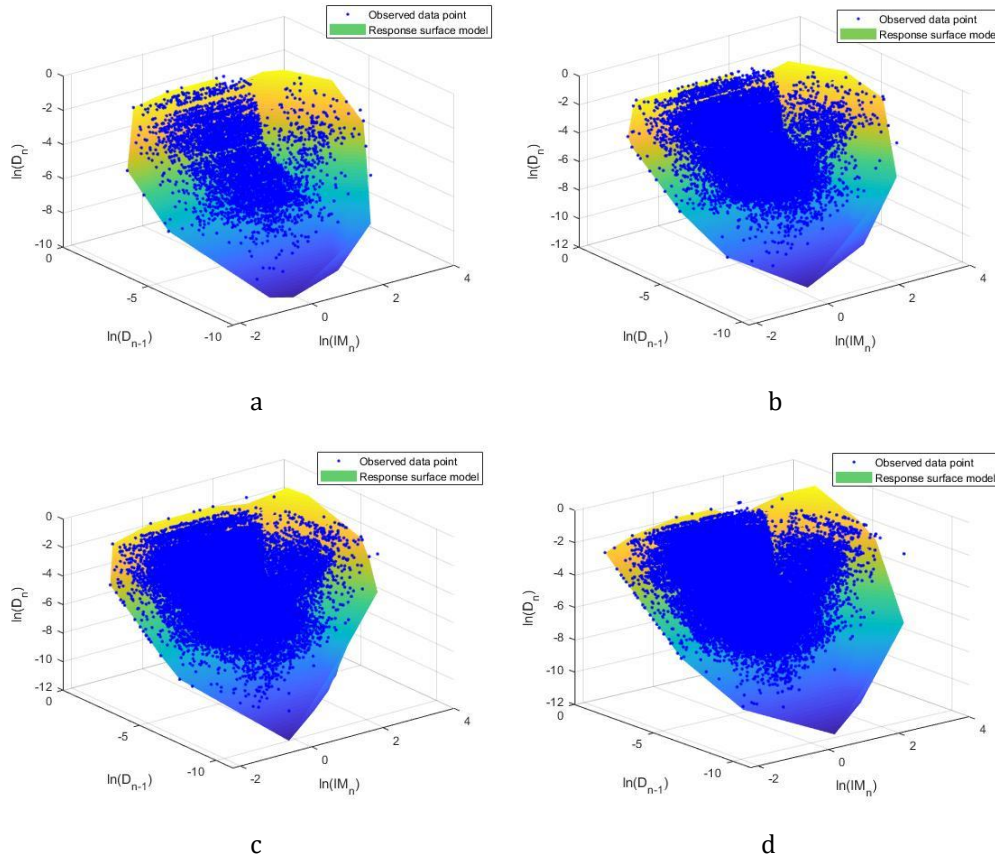


Figure 5.17 Multilinear regression model for predicting the damage index after n shocks as a function of the PGA of the n th shock and the damage index of the previous one. Regression is carried out with an increasing number of samples a)300 b)1000 c)2500 d)3500

Table 14 Regression coefficients and respective RMSE.

Samples	α	β	γ	δ	Sa*[m/s ²]	ϵ_1	ϵ_2
300	-1.36	0.65	1.07	0	4.46	0.26	0.68
1000	-1.97	0.52	1.28	0	4.78	0.29	0.65
2500	-2.1	0.49	1.28	0	4.89	0.29	0.65
3500	-1.68	0.58	1.21	0	4.87	0.27	0.66

COMPUTATION OF EDPs EXCEEDANCE PROBABILITIES

The probability of collapse for an increasing number of occurrences is obtained applying the procedure described in paragraphs 3.2.2

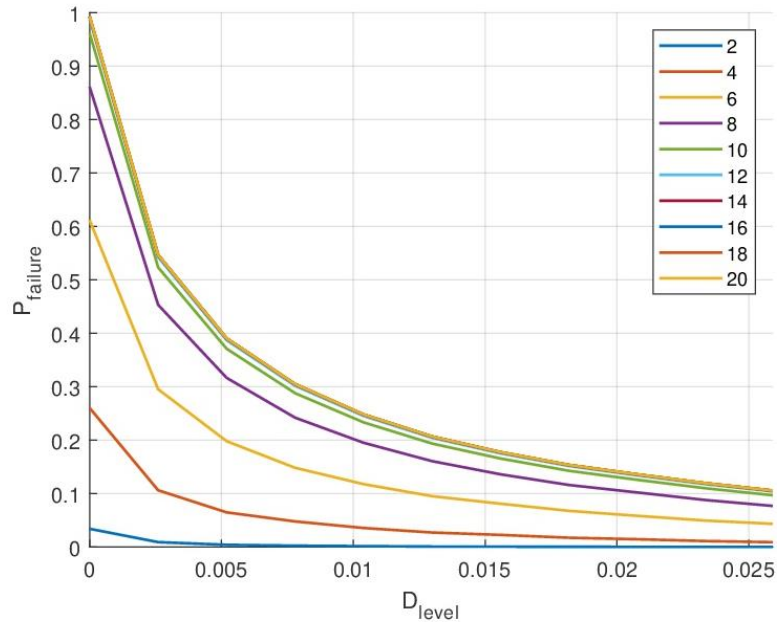


Figure 5.18 Probability of failure with an increasing number of occurrences.

The figure shows that increasing the number of occurrences, the probability of collapse rises considerably reaching, after about twelve earthquakes, the 100% of probability to overcome the first level of damage. We can see that to push the analysis beyond ten occurrences is useless since the curves for a number of earthquakes major than twelve coincide.

CONVERGENCE STUDY

In order to optimize the treatment of Ghosh et al. by minimizing the number of samples to be analysed, a convergence study was performed. The procedures described above were performed with an increasing number of randomly extracted samples. The aim was to understand the number of samples beyond which it was not useful to push the analyses. The results of this study are visible in the figure 5.18.

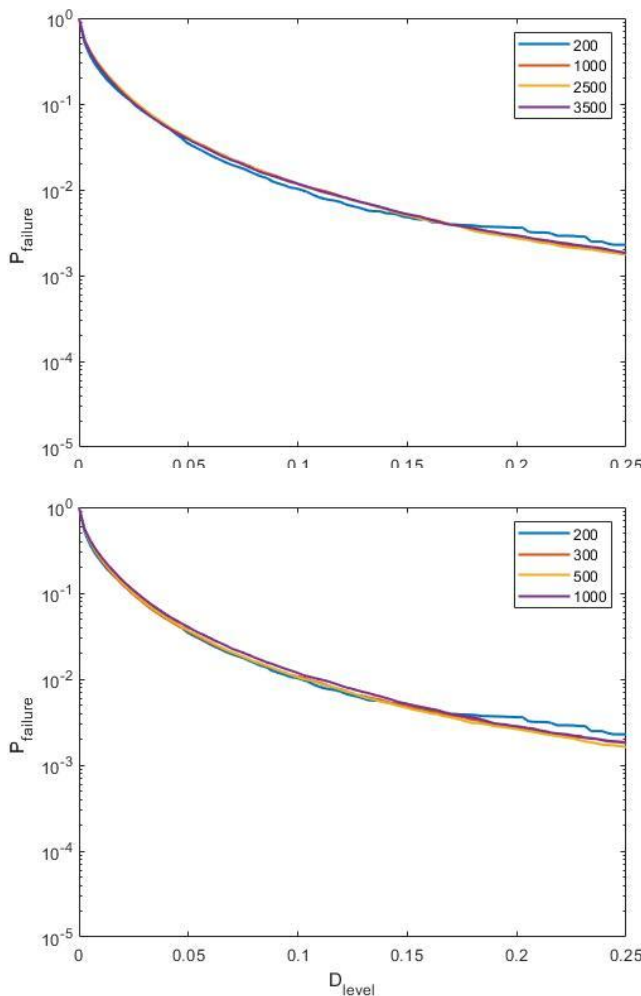


Figure 5.19 Probability of failure evaluated with an increasing number of samples.

In the first instance the following cases were studied: 200, 1000, 2500 and 3000 samples. It was then realized that over 1000 the solutions coincided so it was useless to go beyond this value. Therefore, we sought values in the range between 200 and 1000 that would allow the analysis to be lightened without affecting its quality. The study was conducted for 300 and

500 samples, leading to the conclusion that by choosing a population of 300 samples we can optimize the results.

5.3.1.5 Maximum strain of steel under compression

In this research the Dhakal and Maekawa buckling model is used for modelling the post-yield buckling behaviour of corroded reinforcing bars. In this model, the post-yield buckling response of reinforcement is defined as shown in the next figure:

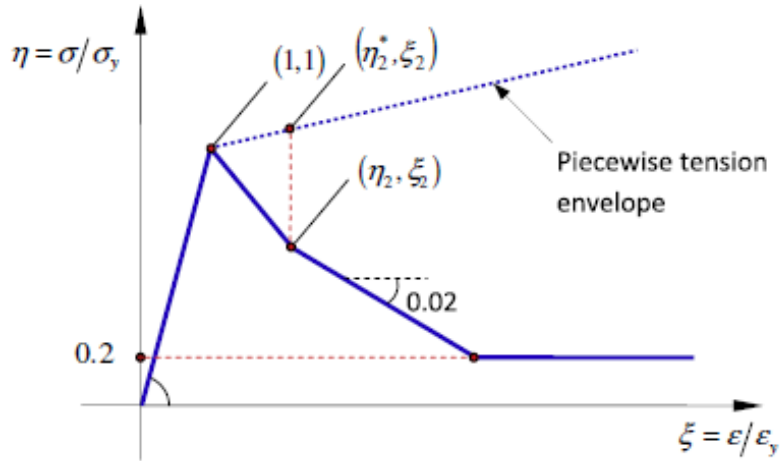


Figure 5.20 Cyclic response of steel reinforcement model under compression, employed in the analyses

Failure may occur due to exceeding the maximum compressive strength and/or exceeding the maximum relative strain. In this case the maximum admissible deformation is 0.08.

LINEAR REGRESSION

Looking at the figures it is possible to see that, despite the results from the analyses are very dispersed, the regression is quite good as shown by the value of the standard deviation of residuals (root mean square error) which leans towards zero. In the footer table the values of the regression coefficients are summarized with the respective errors.

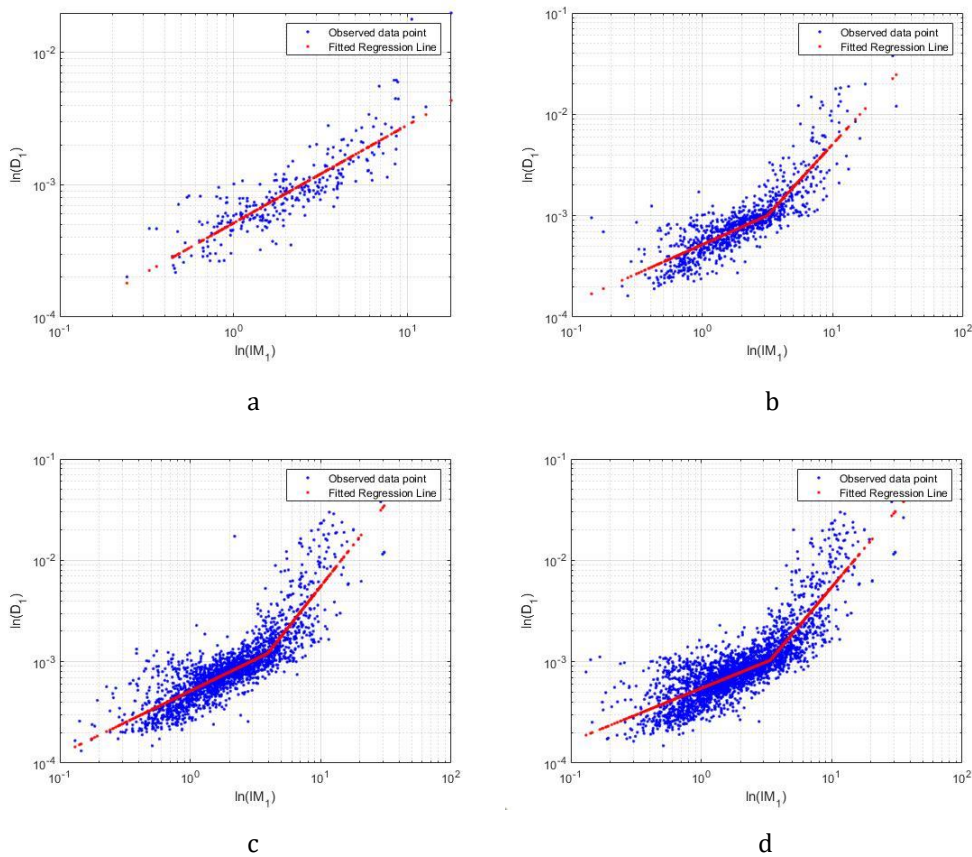


Figure 5.21 Linear regression model for predicting the damage index following single shock. Regression is carried out with an increasing number of samples a)300 b)1000 c)2500 d)3500

Table 15 Regression coefficients and RMSE.

Samples	α	β	γ	Sa*[m/s ²]	ϵ_1	ϵ_2
300	-7.57	0.74	0.68	---	0.35	---
1000	-7.56	0.57	1.4	3.14	0.30	0.52
2500	-7.57	0.62	1.63	3.92	0.31	0.62
3500	-7.51	0.52	1.53	3.37	0.32	0.58

MULTILINEAR REGRESSION

The regression surface seems to approximate very well the course of damage resulting from the analysis. It can be seen how increasing the number of samples significantly does not significantly improve the quality of the regression therefore, we will try to find the minimum number of samples that guarantees acceptable results.

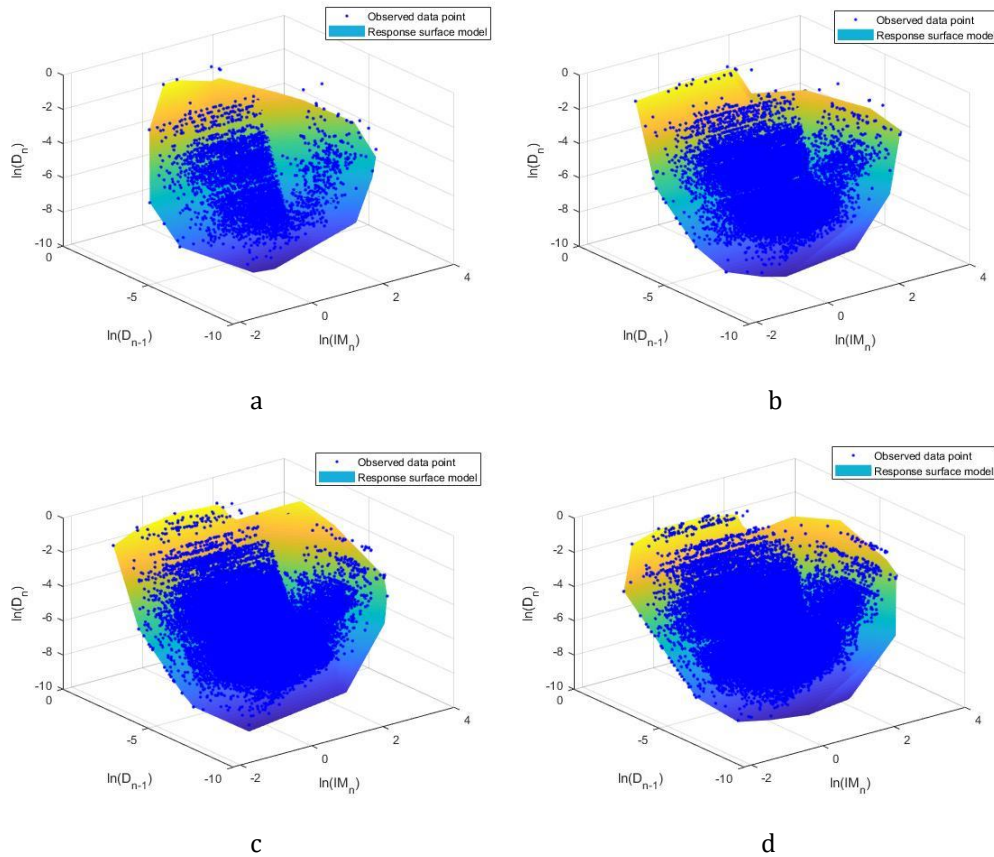


Figure 5.22 Multilinear regression model for predicting the damage index after n shocks as a function of the PGA of the n th shock and the damage index of the previous one. Regression is carried out with an increasing number of samples a)300 b)1000 c)2500 d)3500

Table 16 Regression coefficients and RMSE.

Samples	α	β	γ	δ	$Sa^* [m/s^2]$	ϵ_1	ϵ_2
300	-1.25	0.80	0.66	0	2.39	0.08	0.44
1000	-2.36	0.56	1.33	0	5.35	0.18	0.60
2500	-1.43	0.69	1.29	0	6.04	0.20	0.67
3500	-2.31	0.55	1.37	0	5.8	0.19	0.63

COMPUTATION OF EDPs EXCEEDANCE PROBABILITIES

Applying the procedure described in paragraphs 3.2.2, the following curves are obtained:

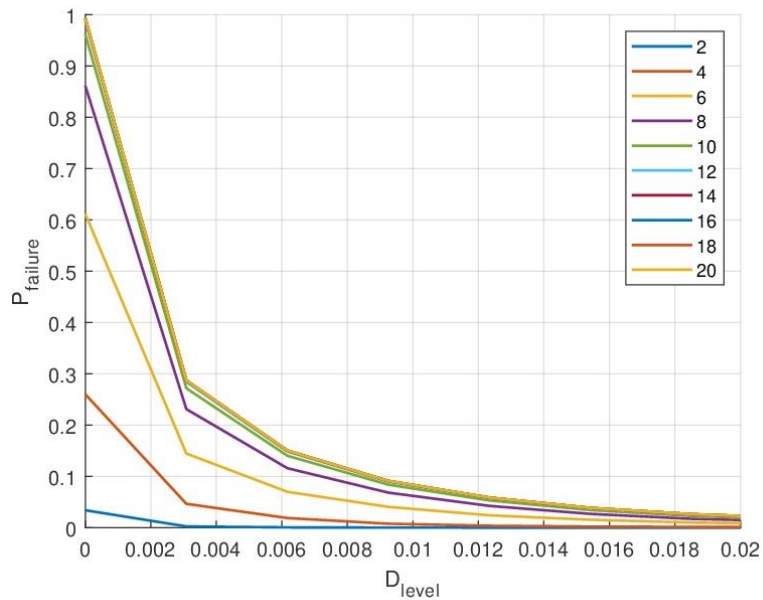


Figure 5.23 Probability of failure with an increasing number of occurrences.

They represent the probability of collapse for an increasing number of occurrences. Increasing the number of occurrences, the probability of collapse rises considerably reaching, after about ten earthquakes, the 100% of probability to overcome the first level of damage. We can see that to push the analysis beyond ten occurrences is useless since the curves for a number of earthquakes major than ten coincide.

CONVERGENCE STUDY

In order to optimize the treatment of Ghosh et al. by minimizing the number of samples to be analysed, a convergence study was performed. The procedures described above were performed with an increasing number of randomly extracted samples. The aim was to understand the number of samples beyond which it was not useful to push the analyses. The results of this study are visible in the Fig. 5.23.

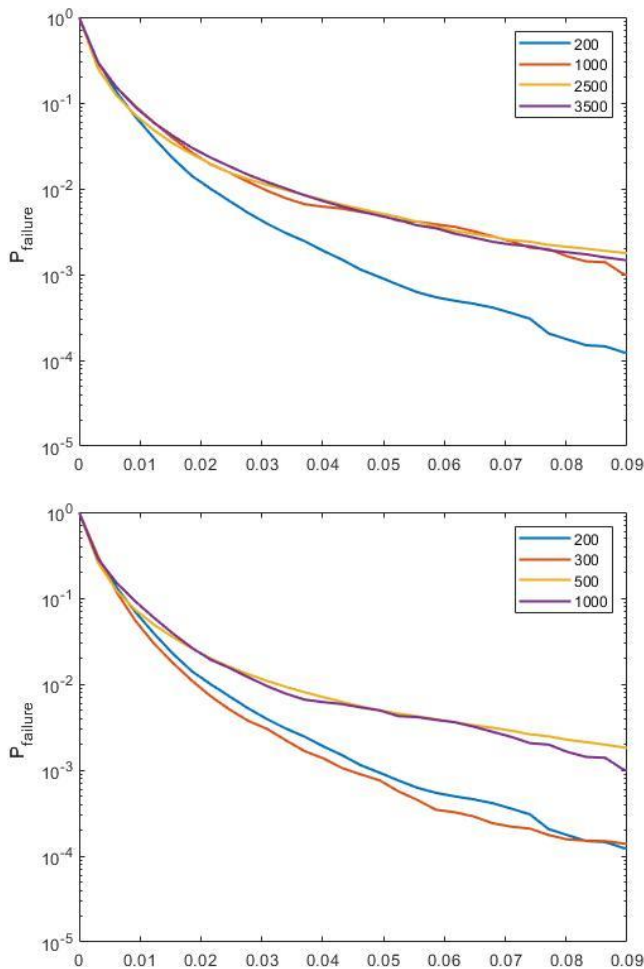


Figure 5.24 Probability of failure evaluated with an increasing number of samples.

In the first instance the following cases were studied: 200, 1000, 2500 and 3000 samples. It was then realized that over 1000 the solutions coincided so it was useless to go beyond this value. Therefore, we sought values in the range between 200 and 1000 that would allow the analysis to be lightened without affecting its quality.

The study was conducted for 300 and 500 samples, leading to the conclusion that by choosing a population of 300 samples we can optimize the results.

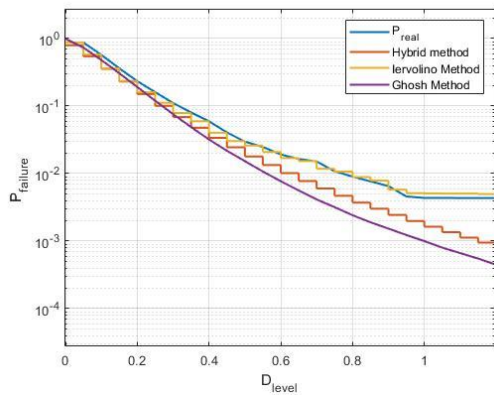
5.3.2 Hybrid method

The application of the different methodologies has allowed us to evaluate the advantages and disadvantages of each ones. During the analysis an idea was born: a hybrid method that combines the strengths of individual approaches. For this reason, it was decided to create a method for evaluating the probability of failure given by the union of the Ghosh regression model and the Iervolino transition matrix. we therefore launched analyses for 300 samples of multiple earthquakes with which we performed the multilinear regression. Using the regression coefficients, a damage matrix was generated for 50,000 cases that served to summarize the transition matrix. The results deriving from the application of this new method are shown in the following paragraph.

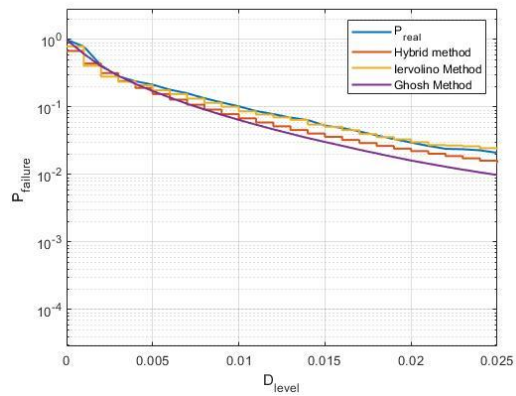
5.3.3 Comparison between different approaches

The previous paragraphs aimed to establish the necessary number of samples to be used in each method to optimize the results and to have an accurate evaluation of the probability of collapse. Once this is laid down, we can proceed to compare the results obtained with the different approaches. The following images show the curves resulting from the application of the methods explained in chapter 3 for each EDPs chosen. As can be seen from the following graphs; the Markovian method and the frequentist one, both based on real results deriving from the analysis, lead to very similar hazard curves. Ghosh method, based on linear and multilinear regression, leads to results that differ from those previously obtained. At the base of the differences that occur in the results there is, probably, that the linear regression fails to capture any anomalous events that are taken into account using the other two

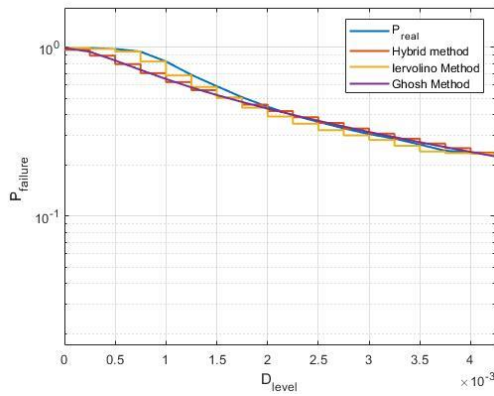
approaches. In any case, a careful analysis of the situation leads us to conclude that; since the probability evaluated by the three methods, although present some differences, leads to similar and equally reliable results; the Ghosh approach is the most useful method because it allows to reduce the number of samples on which to perform the analyses. The so-called hybrid method exploits the Ghosh regressive model that allows a good approximation of the results with a very low number of samples and the Markov transition matrix that characterizes the Iervolino method and that leads us to have results very close to the real ones. The approach is highly competitive but requires further studies and validations that can confirm the results obtained. In the following page you can see the results described up to now.



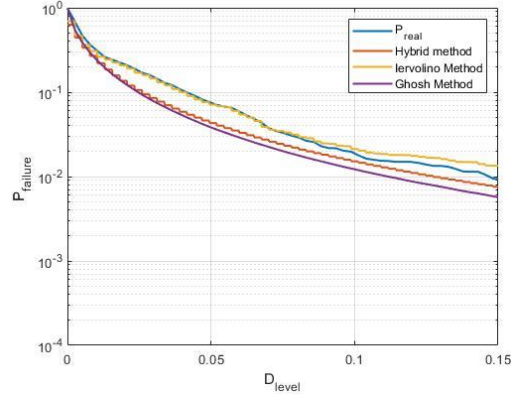
a



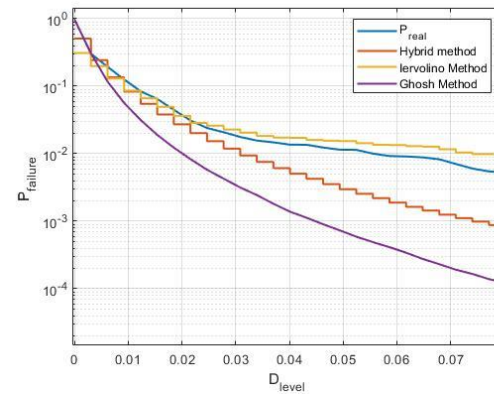
b



c



d



e

Figure 5.25 Probability of failure evaluated with different approaches: Ghosh method, Iervolino Method, frequentist approach and hybrid one for the chosen EPDs (a) Park and Ang index, b) strain of confined concrete under compression c) strain of unconfined concrete under compression and d) tension and e) strain of steel under compression)

5.4 Results of Lehman and Mohel column 1015

5.4.1 Ghosh et al. model

In this case the operations carried out in the previous paragraph on column 815 have been performed on the column 1015 which is slenderer than the previous one. It should be emphasized that, with the same seismic forcing, the second column collapses more often. Nevertheless, the probability of failure assessed for the second column shows very promising results. The results of the work carried out are reported below.

5.4.1.1 Park and Ang damage index

As said before, this damage index is a linear combination between ductility demand and dissipated energy due to earthquake.

Pertinent structural characteristics required for the damage index estimation, are presented in Table 16.

Table 17 Structural characteristic for column 1015

Characteristic	Value
u_u [m]	0.6
u_y [m]	0.06
F_y [kN]	100
β	0.05

The fitted multilinear regression models now follow the form shown in Equation 5-6, conditioned on the PGA intensity of the latest pulse and the damage incurred up to the previous shock. The images below show the results of linear and multilinear regression with the respective regression coefficients, with a number of sampled earthquakes increasing from 300 to 3500.

LINEAR REGRESSION

Strictly speaking, we report the data relating to linear regression. Looking at the figures it is possible to see that, the results from the analyses are very dispersed so regression model need to be improved.

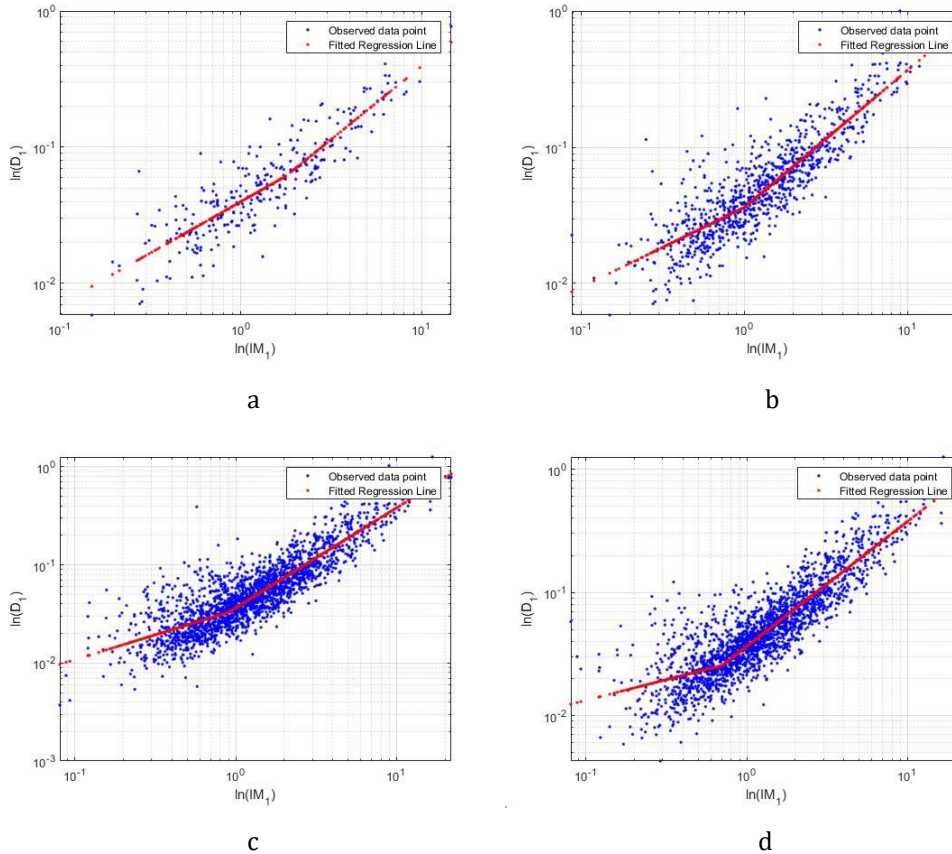


Figure 5.26 Linear regression model for predicting the damage index following single shock. Regression is carried out with an increasing number of samples a)300 b)1000 c)2500 d)3500

In the footer table the values of the regression coefficients are summarized with the respective errors.

Table 18 Regression coefficients and RMSE.

Samples	α	β	γ	Sa*[m/s ²]	ϵ_1	ϵ_2
300	-3.22	0.75	1.07	1.77	0.39	0.34
1000	-3.32	0.58	1.01	1.02	0.41	0.35
2500	-3.36	0.51	1.02	0.91	0.47	0.35
3500	-3.55	0.33	1.02	0.71	0.49	0.35

MULTILINEAR REGRESSION

The regression is quite good but need further studies. It can be seen how increasing the number of samples significantly does not significantly improve the quality of the regression therefore, we will try to find the minimum number of samples that guarantees acceptable results.

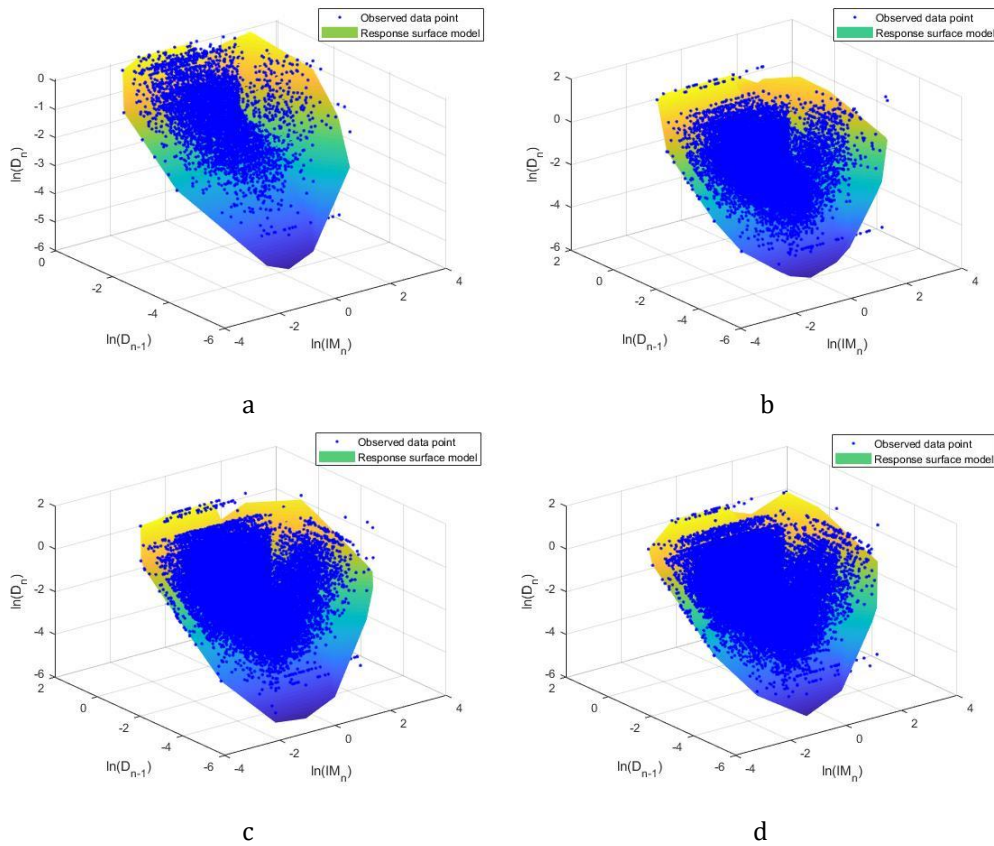


Figure 5.27 Multilinear regression model for predicting the damage index after n shocks as a function of the PGA of the n th shock and the damage index of the previous one. Regression is carried out with an increasing number of samples a)300 b)1000 c)2500 d)3500

Table 19 Regression coefficients and RMSE.

Samples	α	β	γ	δ	Sa*[m/s ²]	ϵ_1	ϵ_2
300	-0.75	0.49	0.53	0	2.88	0.17	0.34
1000	-0.73	0.514	0.58	0	2.9	0.17	0.34
2500	-0.67	0.57	0.54	0	2.47	0.16	0.33
3500	-0.74	0.50	0.59	0	2.88	0.17	0.35

COMPUTATION OF DAMAGE INDEX EXCEEDANCE PROBABILITIES

Applying the procedure described in paragraphs 3.2.2, the following curves are obtained:

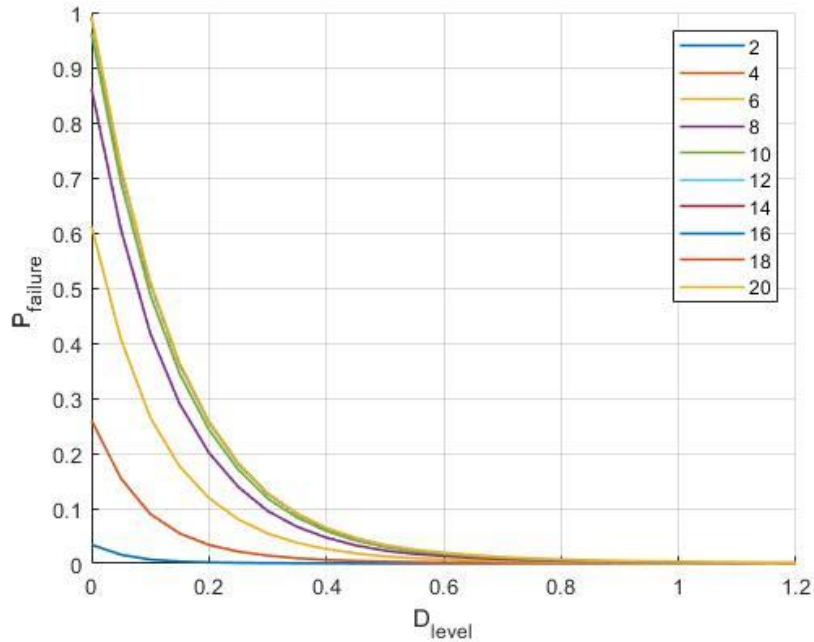


Figure 5.28 Probability of failure with an increasing number of occurrences.

They represent the probability of collapse for an increasing number of occurrences. Increasing the number of occurrences, the probability of collapse rises considerably reaching, after about ten earthquakes, the 100% of probability to overcome the first level of damage. We can see that to push the analysis beyond ten occurrences is useless since the curves for a number of earthquakes major than ten coincide.

CONVERGENCE STUDY

The results of the analyses for an increasing number of intensity measures are shown below. The aim of this work is evaluate the minimum number of samples that grant good accuracy in the regression.

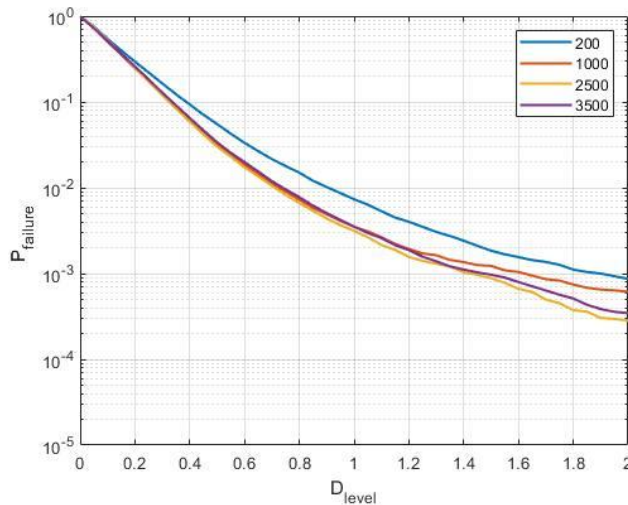
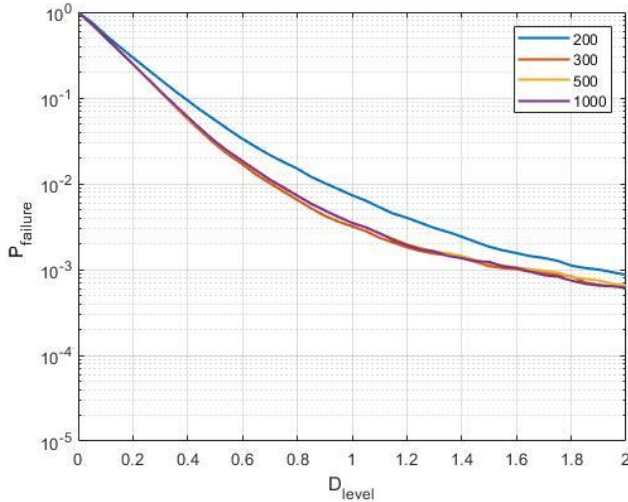


Figure 5.29 Probability of failure evaluated with an increasing number of samples.

In the first instance the following cases were studied: 200, 1000, 2500 and 3000 samples. It was then realized that over 1000 the solutions coincided so it was useless to go beyond this value. Therefore, we

sought values in the range between 200 and 1000 that would allow the analysis to be lightened without affecting its quality. The study was conducted for 300 and 500 samples, leading to the conclusion that by

choosing a population of 300 samples we can optimize the results.

5.4.1.2 Maximum strain of confined concrete under compression

The confined concrete is modelled using the confinement parameters developed by Mander et al. The following figure shows the confined and unconfined concrete models with unloading-reloading cycling rules.

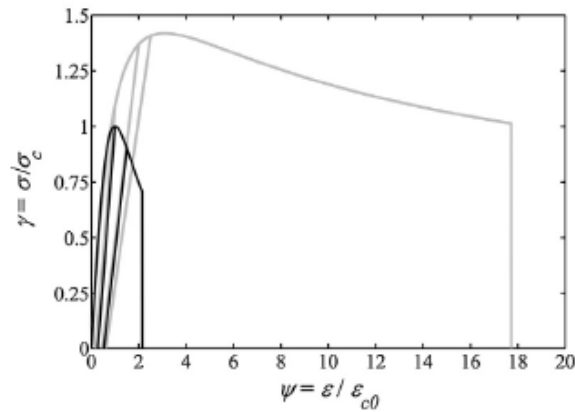


Figure 5.30 Cyclic response of confined concrete model under compression, employed in the analyses

Concrete failure may occur due to exceeding the maximum compressive strength and/or exceeding the maximum relative strain. In this case the maximum admissible deformation is 0.035.

LINEAR REGRESSION

For this parameter we can make similar considerations to the previous ones.

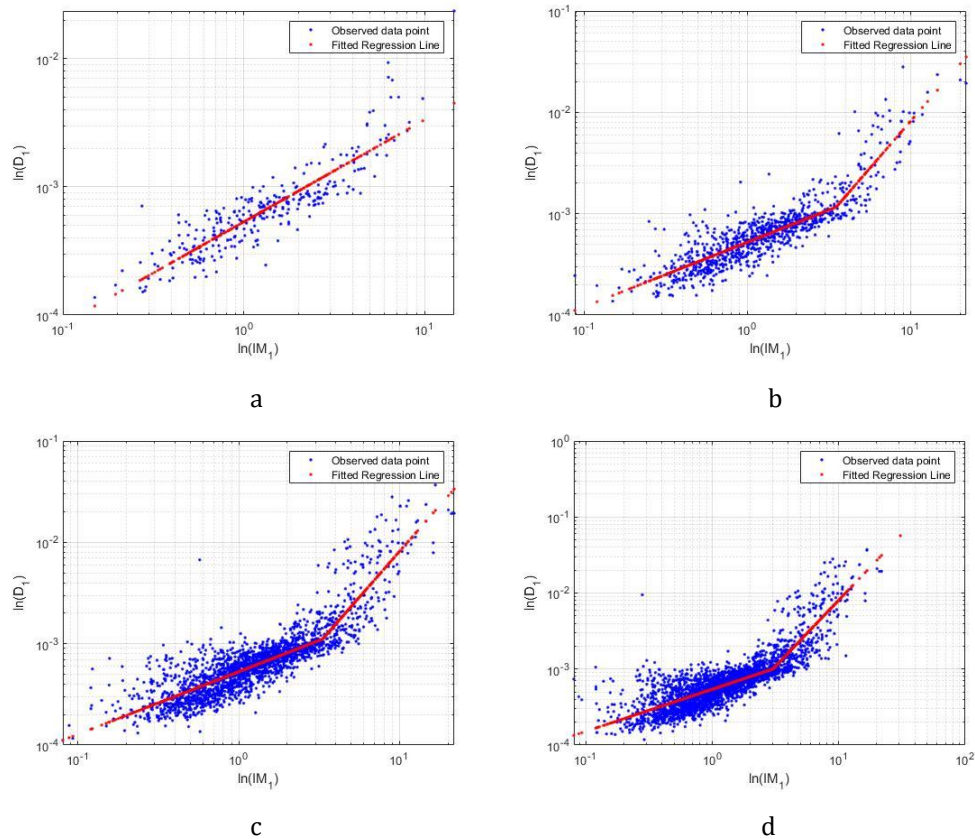


Figure 5.31 Linear regression model for predicting the damage index following single shock. Regression is carried out with an increasing number of samples a)300 b)1000 c)2500 d)3500

Table 20 Regression coefficients and RMSE.

Samples	α	β	γ	Sa*[m/s²]	ϵ_1	ϵ_2
300	-7.49	0.81	0.79	0.11	0	0.34
1000	-7.55	0.63	1.86	3.49	0.29	0.53
2500	-7.54	0.61	1.80	3.32	0.31	0.58
3500	-7.51	0.55	1.73	3.01	0.37	0.51

MULTILINEAR REGRESSION

Thanks to the current regression model it is possible to reach a good level of approximation but, further analysis is needed in order to improve the regression and minimize the present error.

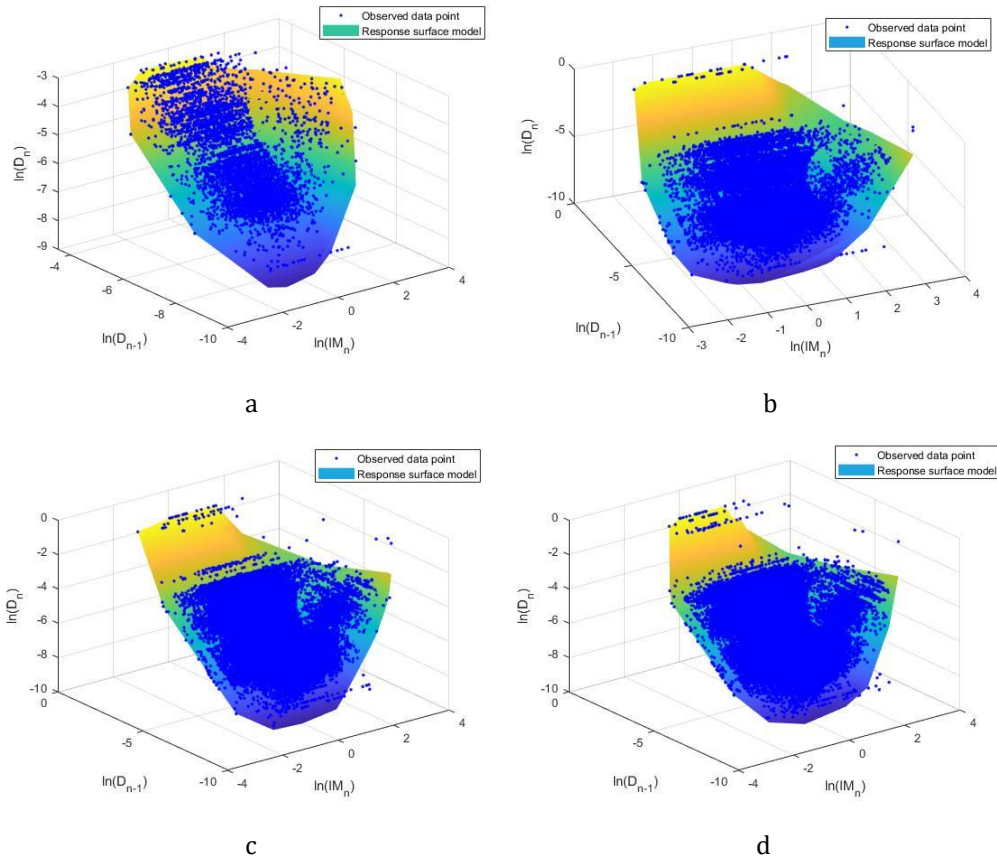


Figure 5.32 Multilinear regression model for predicting the damage index after n shocks as a function of the PGA of the n th shock and the damage index of the previous one. Regression is carried out with an increasing number of samples a)300 b)1000 c)2500 d)3500

Table 21 Regression coefficients and RMSE.

Samples	α	β	γ	δ	Sa*[m/s²]	ϵ_1	ϵ_2
300	-1.11	0.79	-2.18	-0.5	3.35	0.51	0.11
1000	-1.01	0.81	-2.04	-0.53	3.65	0.53	0.17
2500	-1.04	0.81	-2.02	-0.53	3.67	0.52	0.17
3500	-1.02	0.81	-1.93	-0.51	3.52	0.52	0.16

COMPUTATION OF EDPs EXCEEDANCE PROBABILITIES

As for the other EDPs also in this case we have applied the procedure described in paragraphs 3.2.2, the following curves are obtained:

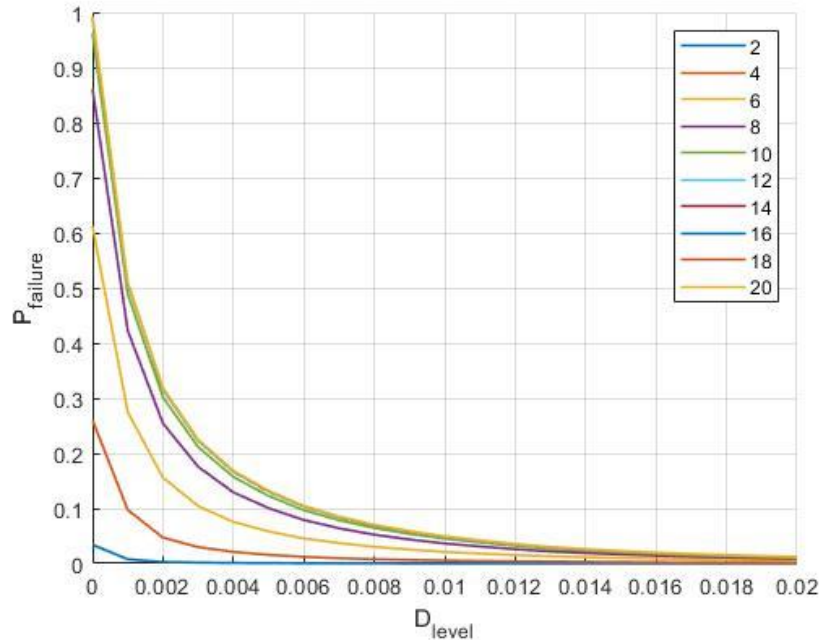


Figure 5.33 Probability of failure with an increasing number of occurrences.

They represent the probability of collapse for an increasing number of occurrences. Increasing the number of occurrences, the probability of collapse rises considerably reaching, after about ten earthquakes, the 100% of probability to overcome the first level of damage. We can see that to push the analysis beyond ten occurrences is useless since the curves for a number of earthquakes major than ten coincide.

CONVERGENCE STUDY

The same procedure of the previous cases is applied.

The study was conducted an increasing number of samples, leading to the conclusion that by choosing a population of 300 samples we can optimize the results.

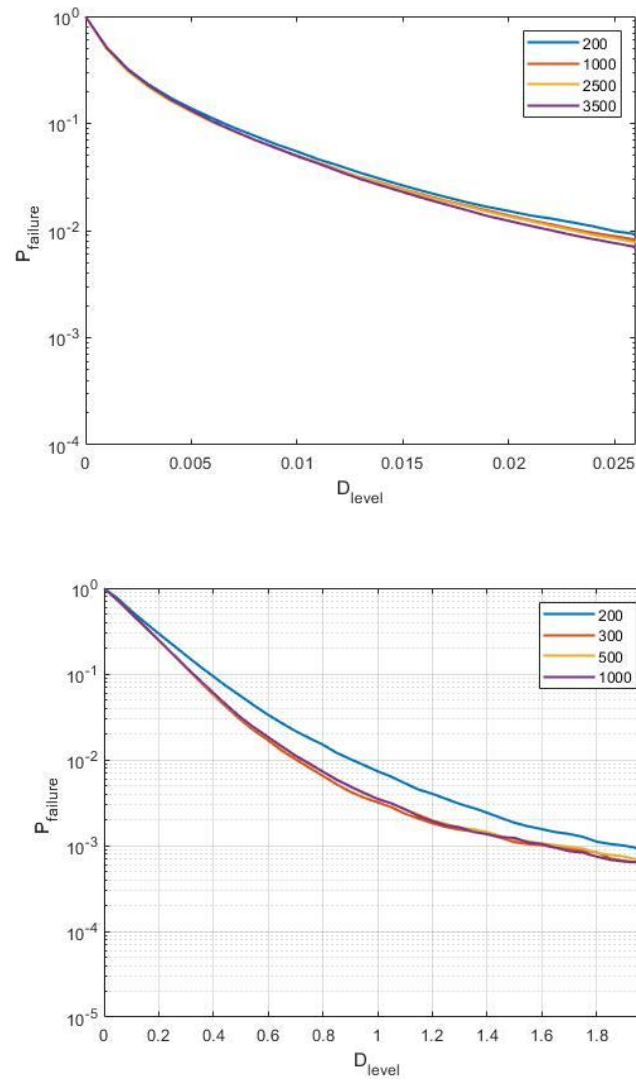


Figure 5.34 Probability of failure evaluated with an increasing number of samples.

5.4.1.3 Maximum strain of unconfined concrete under compression

The unconfined concrete is modelled using the confinement parameters developed by Mander et al. The following figure shows the confined and unconfined concrete models with unloading–reloading cycling rules.

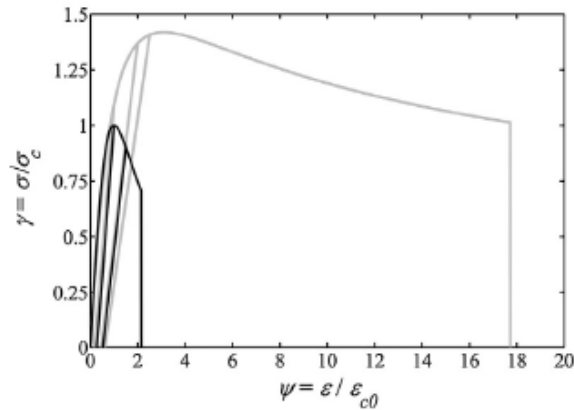


Figure 5.35 Cyclic response of unconfined concrete model under compression, employed in the analyses

Concrete failure may occur due to exceeding the maximum compressive strength and/or exceeding the maximum relative strain. In this case the maximum admissible deformation is 0.00428.

LINEAR REGRESSION

Similar considerations can also be made for concrete not confined in compression. The following images are a summary of the results obtained.

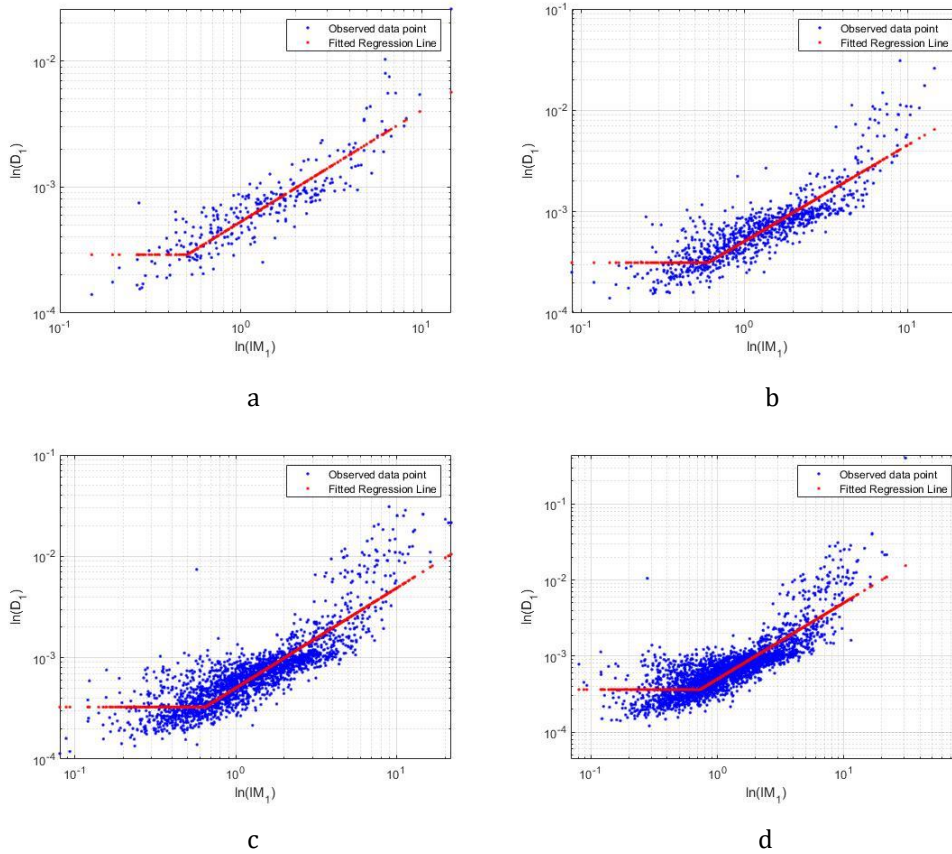


Figure 5.36 Linear regression model for predicting the damage index following single shock. Regression is carried out with an increasing number of samples a)300 b)1000 c)2500 d)3500

Table 22 Regression coefficients and RMSE.

Samples	α	β	γ	Sa*[m/s²]	ϵ_1	ϵ_2
300	-8.43	0.88	-0.68	1	0.33	0.36
1000	-8.07	0.95	-0.51	1	0.36	0.38
2500	-8.02	0.98	-0.44	1	0.37	0.39
3500	-7.92	1.00	-0.31	1	0.41	0.41

MULTILINEAR REGRESSION

Good regression coefficients are estimated, however further consideration should be done to improve regression model and reduce Root mean square errors.

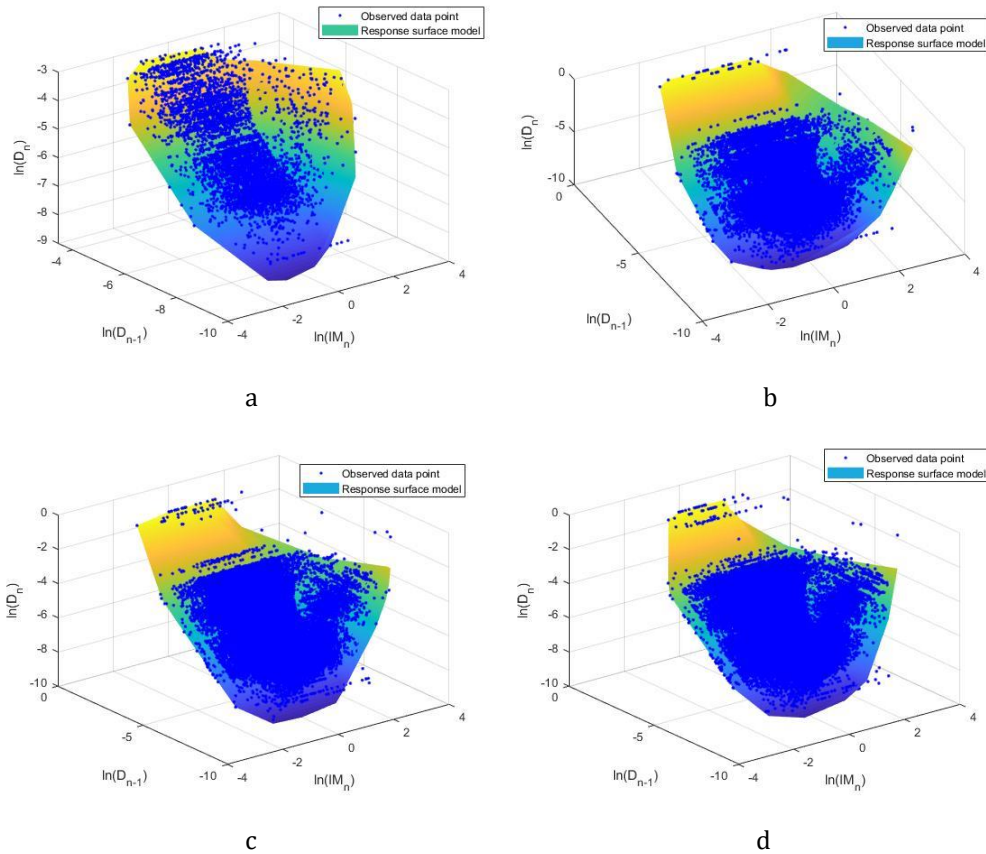


Figure 5.37 Multilinear regression model for predicting the damage index after n shocks as a function of the PGA of the n th shock and the damage index of the previous one. Regression is carried out with an increasing number of samples a)300 b)1000 c)2500 d)3500

In the footer table the values of the regression coefficients are summarized with the respective errors.

Table 23 Regression coefficients and RMSE.

Samples	α	β	γ	δ	$Sa^*[\text{m/s}^2]$	ϵ_1	ϵ_2
300	-1.05	0.81	-2.08	-0.53	3.41	0.16	0.52
1000	-0.95	0.82	-2.01	-0.54	3.55	0.17	0.54
2500	-0.94	0.82	-1.93	-0.51	3.44	0.16	0.52
3500	-0.94	0.83	-1.89	0.51	3.39	0.16	0.52

COMPUTATION OF EDPs EXCEEDANCE PROBABILITIES

The application of Ghosh et al. method for an increasing number of occurrences has brought to the light that it is useless push the analyses beyond 10 occurrences. Indeed, overhead this value the failure probability unchanged by varying the number of occurrences.

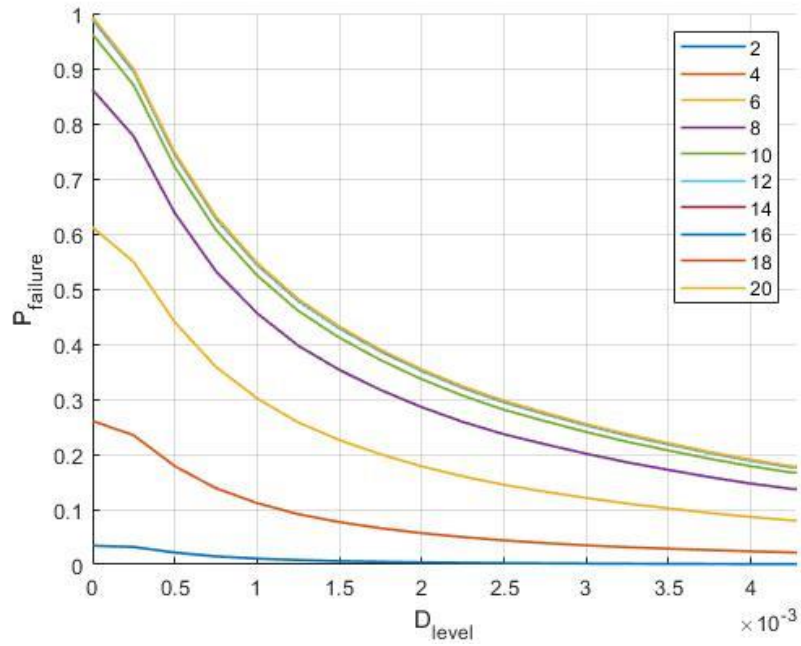


Figure 5.38 Probability of failure with an increasing number of occurrences.

CONVERGENCE STUDY

The results of the convergence study are visible in the Fig. 5.48.

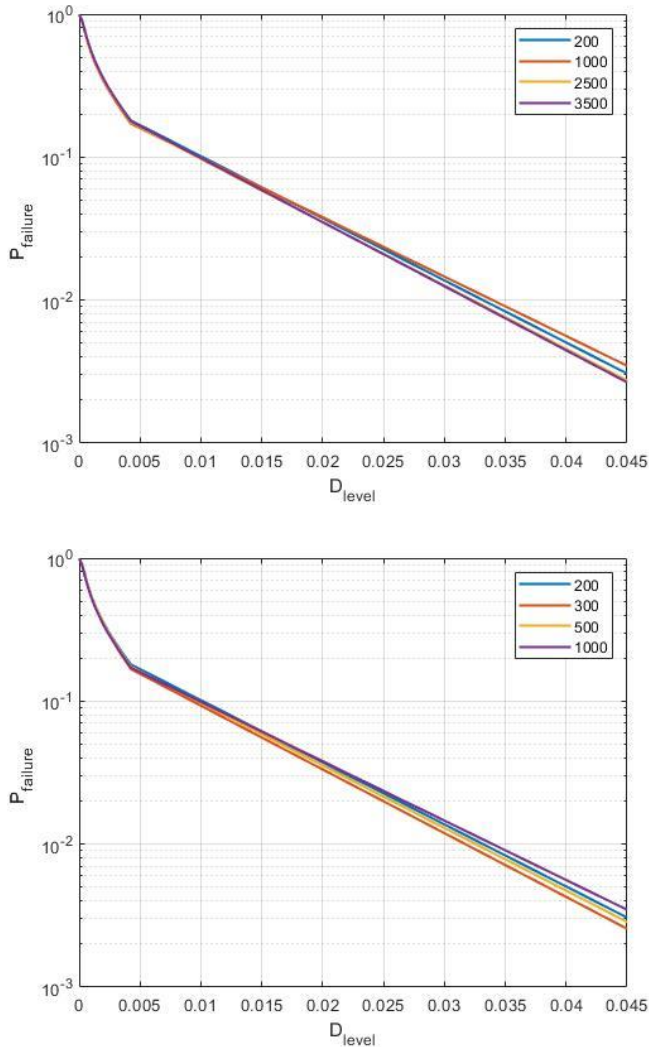


Figure 5.39 Probability of failure evaluated with an increasing number of samples.

In the first instance the following cases were studied: 200, 1000, 2500 and 3000 samples. It was then realized that over 1000 the solutions coincided so it was useless to go beyond this value. Therefore, we sought values in the range between 200 and 1000 that would allow the analysis to be lightened without affecting its quality. The study was conducted for 300 and 500 samples, leading

to the conclusion that by choosing a population of 300 samples we can optimize the results.

5.4.1.4 Maximum strain of unconfined concrete under tension

The confined concrete is modelled using the confinement parameters developed by Mander et al. The following figure shows the concrete model in tension with unloading–reloading cycling rules.

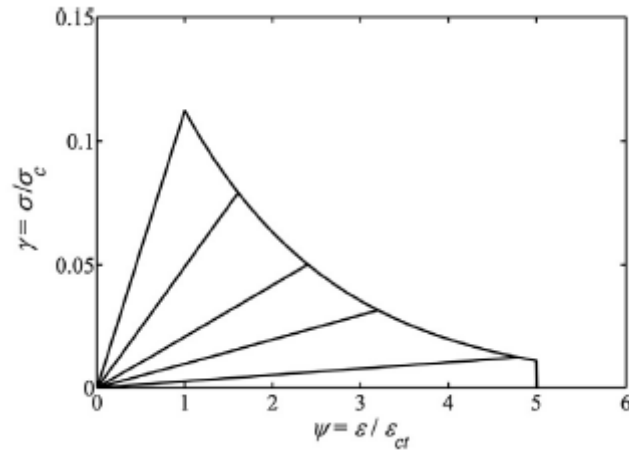


Figure 5.40 Cyclic response of unconfined concrete model under tension, employed in the analyses

Concrete failure may occur due to exceeding the maximum tensile strength and/or exceeding the maximum relative strain. In this case the maximum admissible deformation is 0.00125.

LINEAR REGRESSION

The results of linear regression are shown below. As we can see there is quite high dispersion so

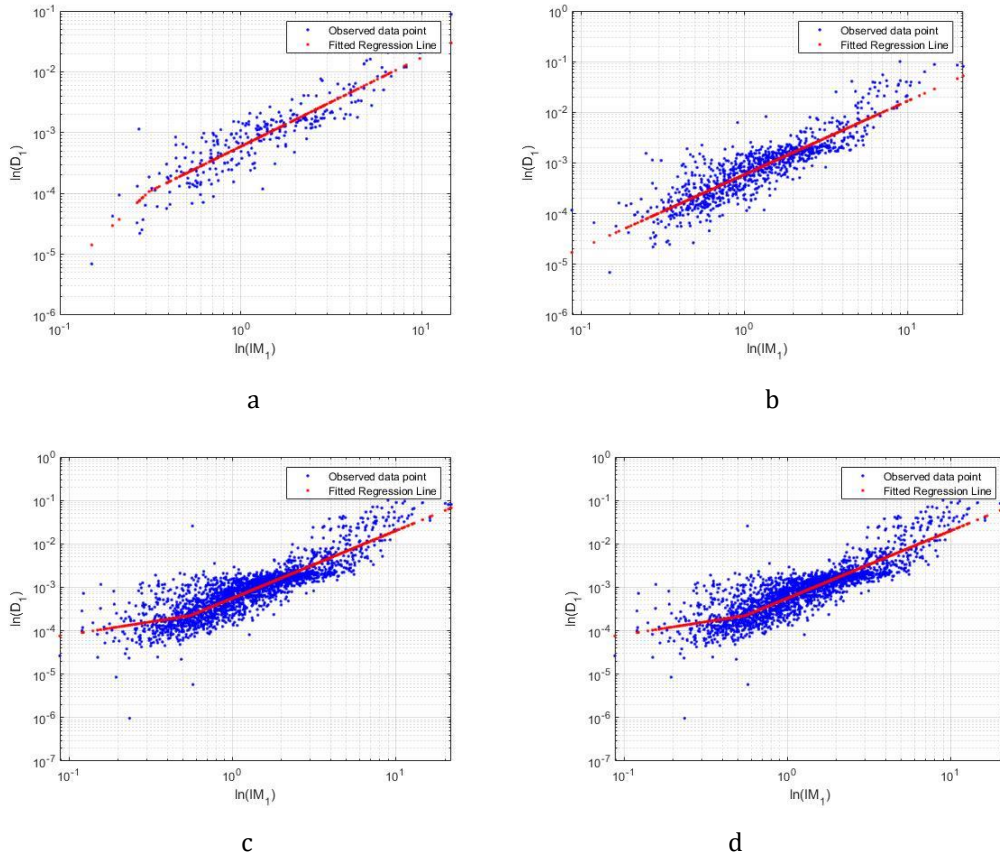


Figure 5.41 Linear regression model for predicting the damage index following single shock. Regression is carried out with an increasing number of samples a)300 b)1000 c)2500 d)3500

Table 24 Regression coefficients and RMSE.

Samples	α	β	γ	Sa*[m/s ²]	ϵ_1	ϵ_2
300	-8.26	1.29	-0.56	1	0.76	0.52
1000	-8.3	1.43	-0.46	1	0.8	0.55
2500	-8.39	1.46	-0.48	1	0.82	0.59
3500	-8.12	1.4	-0.36	1	0.89	0.59

MULTILINEAR REGRESSION

The regression surface seems to approximate very well the course of damage resulting from the analysis. In the next paragraph we will try to find the minimum number of samples that guarantees acceptable results.

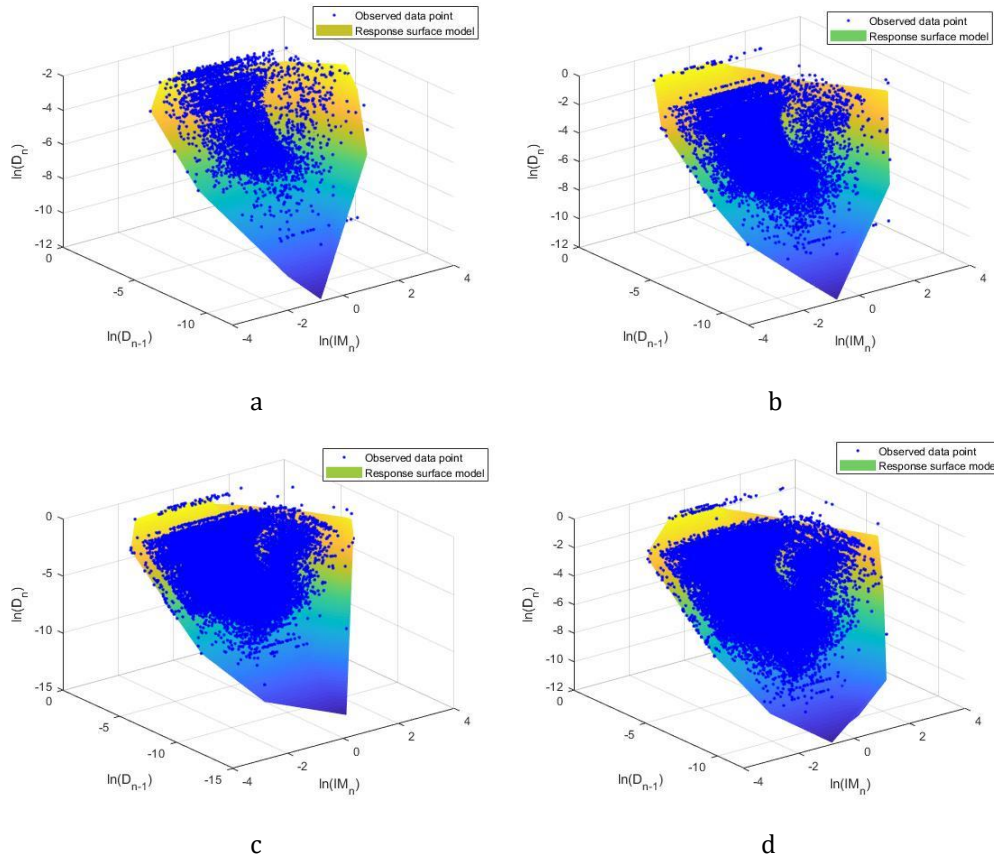


Figure 5.42 Multilinear regression model for predicting the damage index after n shocks as a function of the PGA of the n th shock and the damage index of the previous one. Regression is carried out with an increasing number of samples a)300 b)1000 c)2500 d)3500

In the footer table the values of the regression coefficients are summarized with the respective errors.

Table 25 Regression coefficients and RMSE.

Samples	α	β	γ	δ	$Sa^* [m/s^2]$	ϵ_1	ϵ_2
300	-1.36	0.65	1.07	0	4.46	0.26	0.68
1000	-1.96	0.52	1.28	0	4.78	0.29	0.65
2500	-2.1	0.49	1.28	0	4.89	0.29	0.66
3500	-1.68	0.58	1.21	0	4.83	0.28	0.66

COMPUTATION OF EDPs EXCEEDANCE PROBABILITIES

Applying the procedure described in paragraphs 3.2.2, the following curves are obtained:

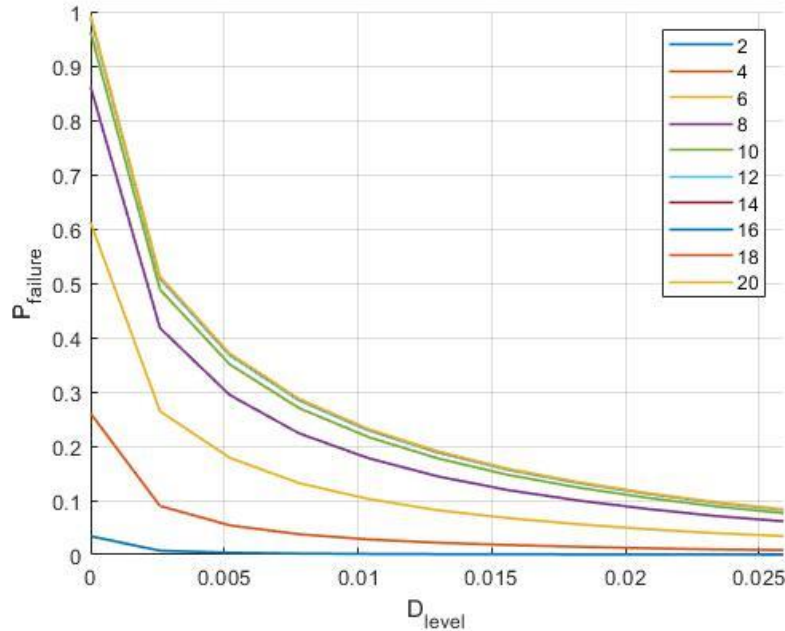


Figure 5.43 Probability of failure with an increasing number of occurrences.

They represent the probability of collapse for an increasing number of occurrences. Increasing the number of occurrences, the probability of collapse rises considerably reaching, after about ten earthquakes, the 100% of probability to overcome the first level of damage. We can see that to push the analysis beyond ten occurrences is useless since the curves for a number of earthquakes major than ten coincide.

CONVERGENCE STUDY

In order to optimize the treatment of Ghosh et al. by minimizing the number of samples to be analysed, a convergence study was performed. The procedures described above were performed with an increasing number of randomly extracted samples. The aim was to understand the number of samples beyond which it was not useful to push the analyses. The results of this study are visible in the Fig. 5.53.

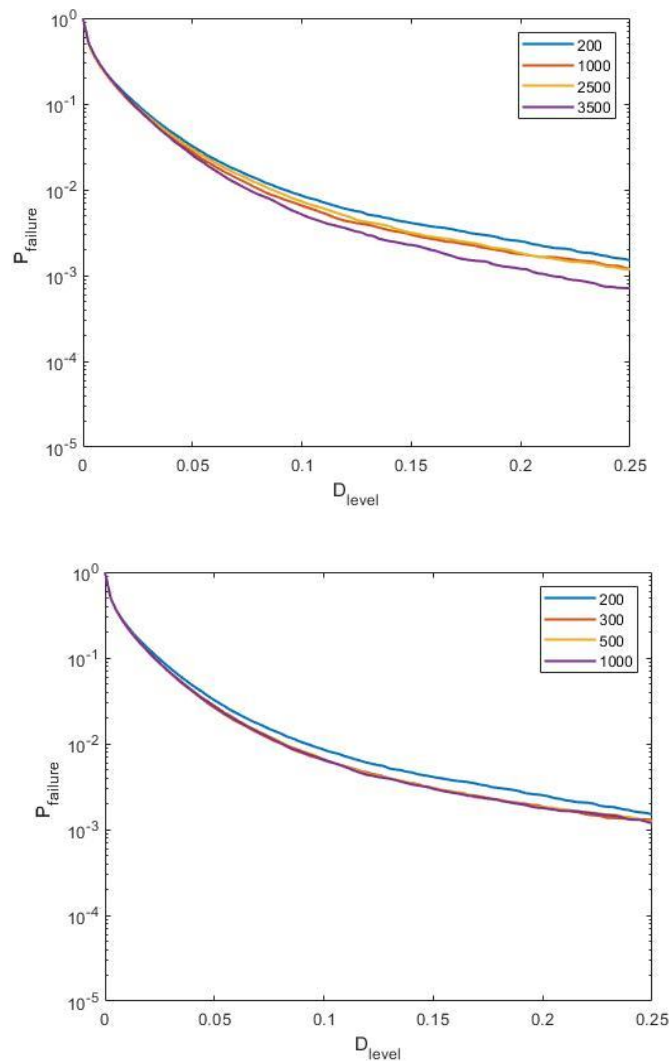


Figure 5.44 Probability of failure evaluated with an increasing number of samples

From the figure we can see that the minimum number of samples that grants good approximation of results is 300.

5.4.1.5 Maximum strain of steel under compression

In this research the Dhakal and Maekawa buckling model is used for modelling the post-yield buckling behaviour of corroded reinforcing bars. In this model, the post-yield buckling response of reinforcement is defined as shown in the next figure:

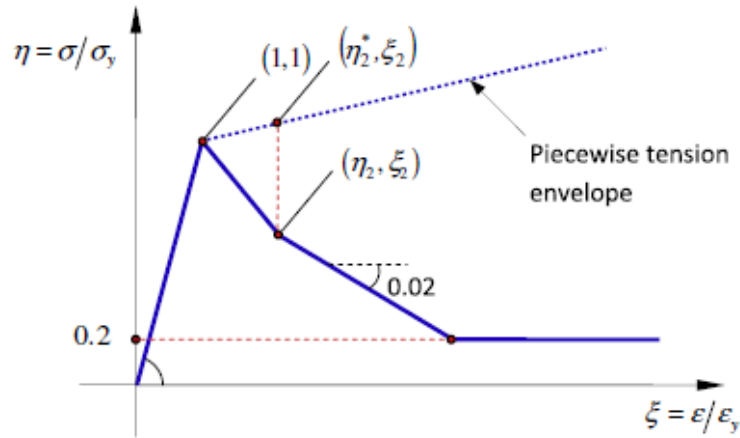


Figure 5.45 Cyclic response of steel reinforcement model under compression, employed in the analyses

Failure may occur due to exceeding the maximum compressive strength and/or exceeding the maximum relative strain. In this case the maximum admissible deformation is 0.086.

LINEAR REGRESSION

Looking at the figures it is possible to see that, despite the results from the analyses are very dispersed, the regression is quite good as shown by the value of the standard deviation of residuals (root mean square error) which leans towards zero. In the footer table the values of the regression coefficients are summarized with the respective errors.

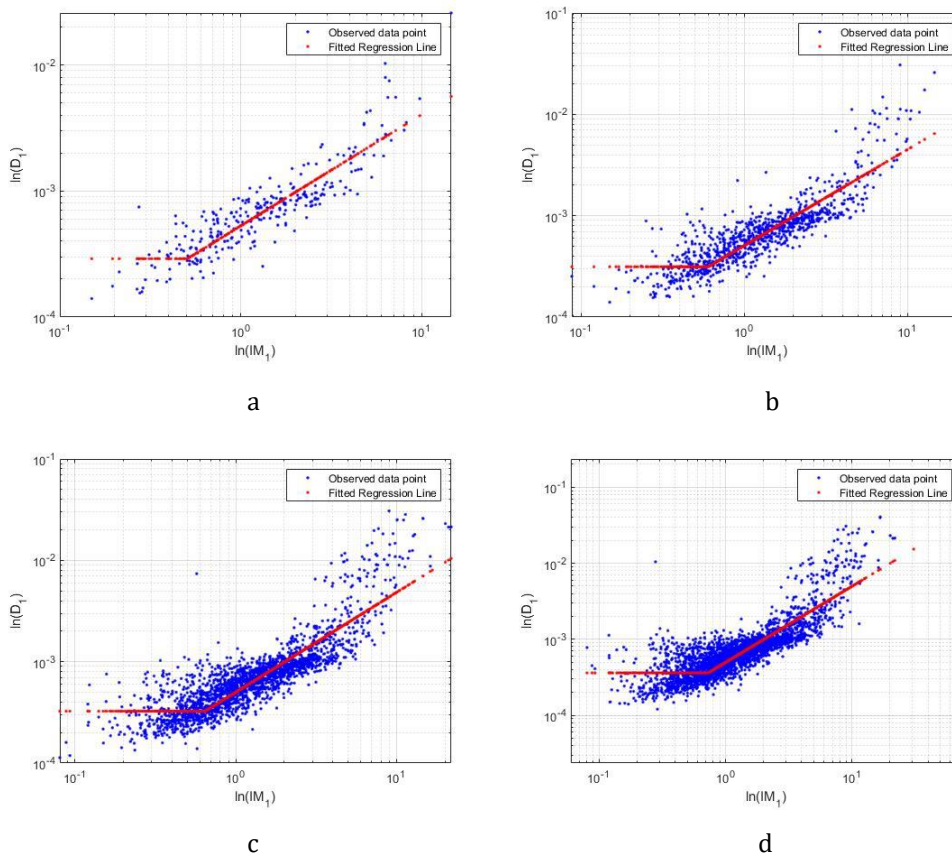


Figure 5.46 Linear regression model for predicting the damage index following single shock. Regression is carried out with an increasing number of samples a)300 b)1000 c)2500 d)3500

Table 26 Regression coefficients and RMSE.

Samples	α	β	γ	Sa*[m/s ²]	ϵ_1	ϵ_2
300	-7.57	0.74	0.68	/	0.35	/
1000	-7.56	0.57	1.40	3.14	0.30	0.52
2500	-7.57	0.62	1.63	3.92	0.31	0.63
3500	-7.51	0.52	1.53	3.37	0.32	0.58

MULTILINEAR REGRESSION

The results of the application of predictive equation described in chapter 3 are shown below. As we can see even if the dispersion of samples, there is a good approximation of the trend.

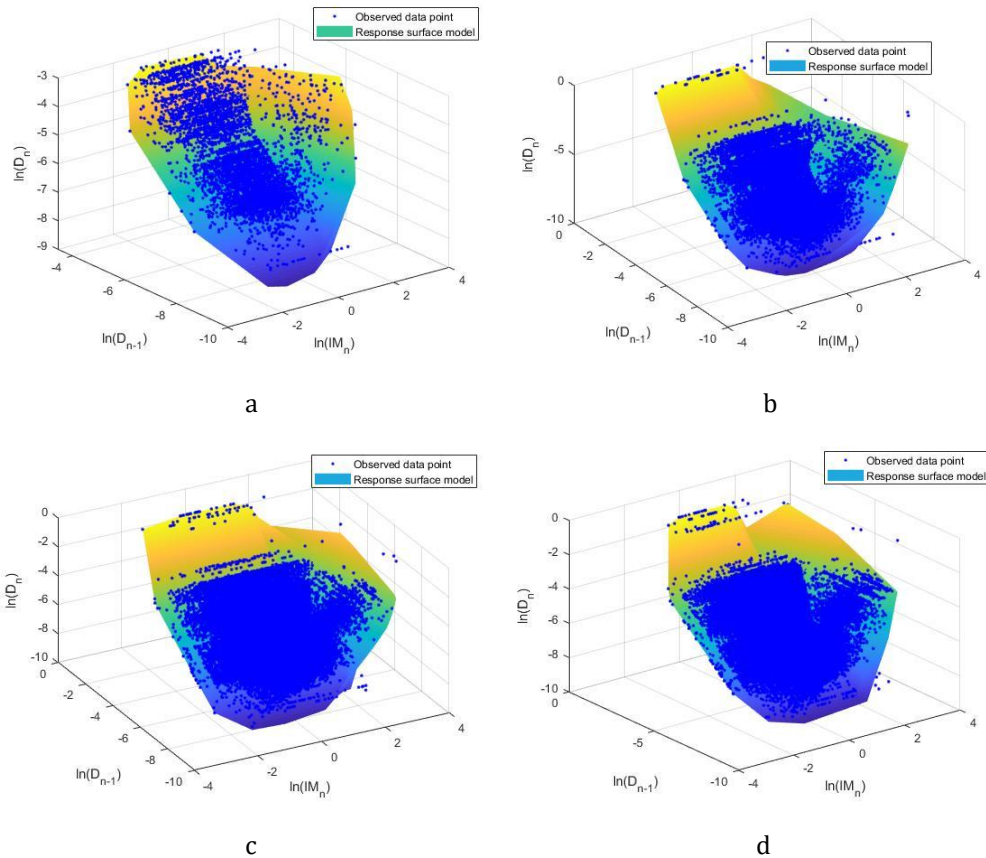


Figure 5.47 Multilinear regression model for predicting the damage index after n shocks as a function of the PGA of the n th shock and the damage index of the previous one. Regression is carried out with an increasing number of samples a)300 b)1000 c)2500 d)3500

Table 27 Regression coefficients and RMSE.

Samples	α	β	γ	δ	$Sa^*[m/s^2]$	ϵ_1	ϵ_2
300	-1.25	0.8	0.66	0	2.31	0.08	0.44
1000	-2.36	0.55	1.39	0	5.35	0.18	0.60
2500	-1.43	0.69	1.29	0	6.05	0.20	0.67
3500	-2.31	0.55	1.37	0	5.81	0.19	0.63

COMPUTATION OF EDPs EXCEEDANCE PROBABILITIES

Applying the procedure described in paragraphs 3.2.2, the following curves are obtained:

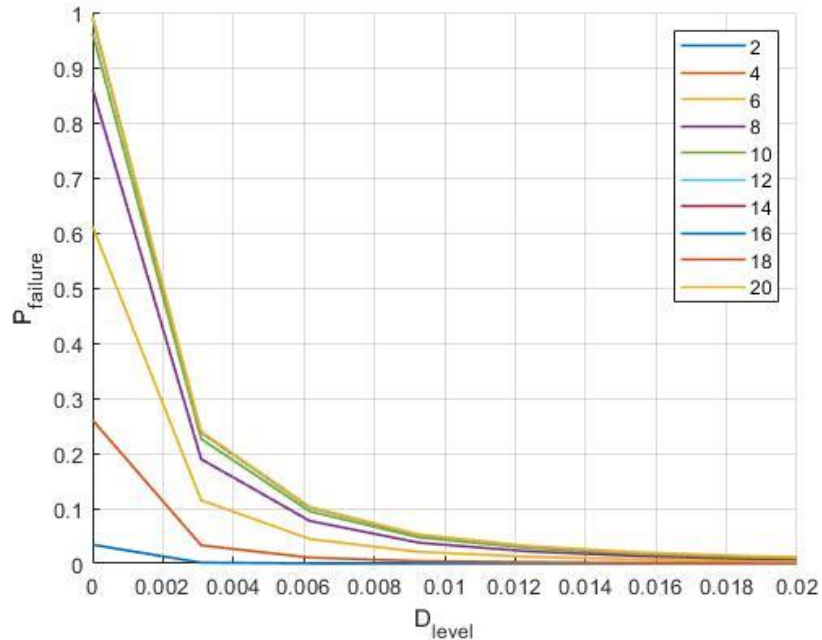
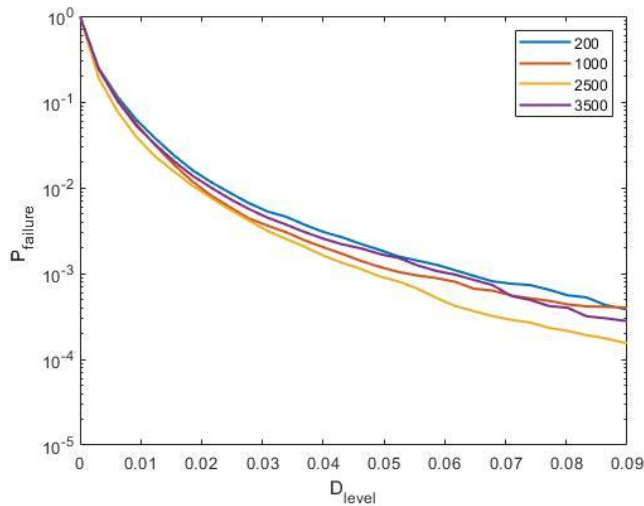


Figure 5.48 Probability of failure with an increasing number of occurrences.

They represent the probability of collapse for an increasing number of occurrences. Increasing the number of occurrences, the probability of collapse rises considerably reaching, after about ten earthquakes, the 100% of probability to overcome the first level of damage. We can see that to push the analysis beyond ten occurrences is useless since the curves for a number of earthquakes major than ten coincide.

CONVERGENCE STUDY

In order to optimize the treatment of Ghosh et al. by minimizing the number of samples to be analysed, a convergence study was performed. The procedures described above were performed with an increasing



number of randomly extracted samples. The aim was to understand the number of samples beyond which it was not useful to push the analyses. The results of this study are visible in the Fig. 5.58.

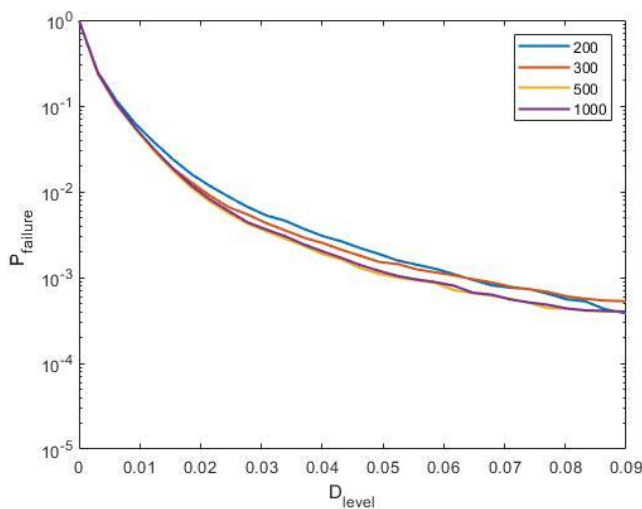


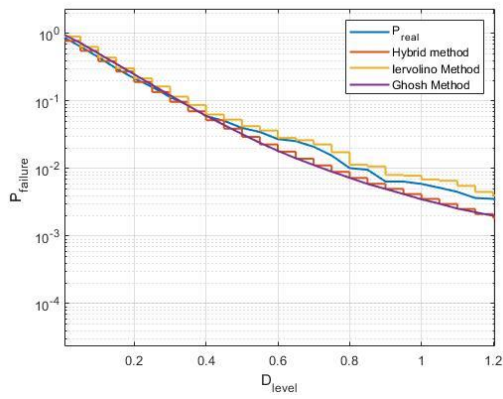
Figure 5.49 Probability of failure evaluated with an increasing number of samples.

In the first instance the following cases were studied: 200, 1000, 2500 and 3000 samples. It was then realized that over 1000 the solutions coincided so it was useless to go beyond this value. Therefore, we

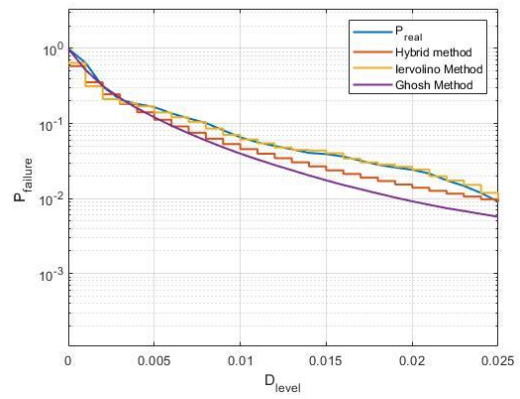
sought values in the range between 200 and 1000 that would allow the analysis to be lightened without affecting its quality. The study was conducted for 300 and 500 samples, leading to the conclusion that by choosing a population of 300 samples we can optimize the results.

5.4.2 Comparison between different approaches

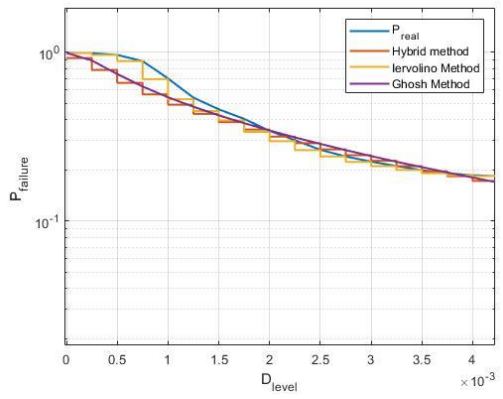
As for column 815 also in the present case, column 1015, the results obtained following the application of the 4 methodologies are shown below. You can see how the Markovian method and the frequentist one, lead to very similar hazard curves. Ghosh method, instead, conducts to results that differ from those previously obtained. At the base of the differences that occur in the results there is, probably, that the linear regression fails to capture any anomalous events that are taken into account using the other two approaches. In any case, a careful analysis of the situation leads us to conclude that; since the probability evaluated by the three methods, although present some differences, leads to similar and equally reliable results; the Ghosh approach is the most useful method because it allows to reduce the number of samples on which to perform the analyses. The so-called hybrid method exploits the Ghosh regressive model that allows a good approximation of the results with a very low number of samples and the Markov transition matrix that characterizes the Iervolino method and that leads us to have results very close to the real ones. The approach is highly competitive but requires further studies and validations that can confirm the results obtained. The results obtained for the second column appear more in line with what we expected. In the following page you can see the results described up to now.



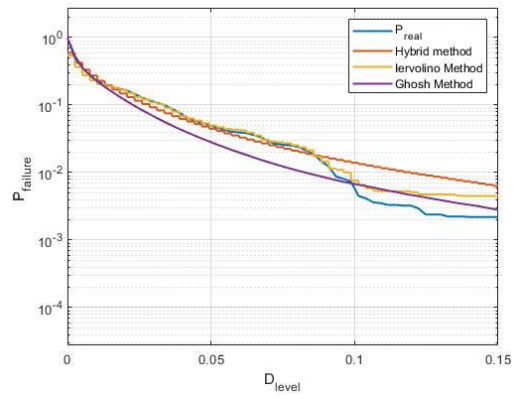
a



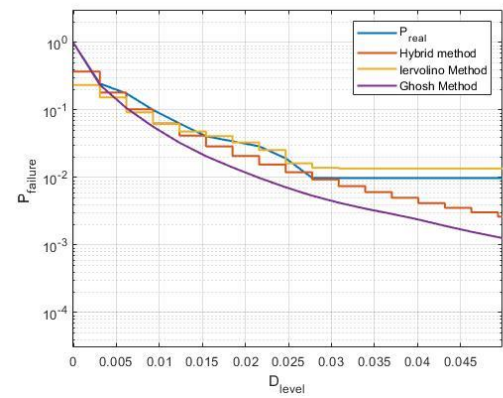
b



c



d



e

Figure 5.50 Probability of failure evaluated with different approaches: Ghosh method, Iervolino Method, frequentist approach and hybrid one for the chosen EPDs (a) Park and Ang index, b) strain of confined concrete under compression c) strain of unconfined concrete under compression and d) tension and e) strain of steel under compression).

6 CONCLUSIONS

It is not yet possible to predict the time and place of environmental disasters such as earthquakes or tsunamis, but it is conceivable to think of directing the current design standards towards a design capable of resisting the harmful effects of the earthquake and limiting human and economic losses. A structure can collapse not only for a single event of considerable magnitude but also because of repeated quakes of minor magnitude that, in the long run, can cause damage accumulation and reduction of structural capacity.

Thus, accumulation process can't be neglected in reliability valuation. The aim of this work is to highlight the importance of taking into account multiple shocks and the subsequent accumulation of damage in seismic design and risk assessment. To reach this goal, an improvement of hazard assessment methodology which relates ground motion to failure probability has been required.

This thesis presents a comparison between existing methodologies for the evaluation of structural earthquake damage under recurrent shocks in order to establish the most efficient and accurate approach.

The research has included the following major activities: critical review of existing bridge damage evaluation procedures; advanced bridge performance analysis using finite element modelling; structural system reliability analysis.

A hybrid method has been also developed; it combines the strengths of each approach previously described and maximizes performance.

The application of the proposed evaluation framework to the introduced structural model allows us to conclude that; although the Ghosh model presents divergences with respect to the probability assessed by mean

of Frequentist method, these differences are not such as to invalidate the goodness of the results.

In the light of the foregoing, it can be concluded that among the existing methodologies, Ghosh is undoubtedly the most advantageous as it requires less computational burden. The hybrid approach combines the advantages linked to the application of the Ghosh method with the greater accuracy deriving from the Markovian one, but it needs further studies and validations that could confirm the results obtained.

However, this research project must be considered as the incipit of a complex in-depth study, able to generate a realistic and reliable estimation of hazard scenarios, thanks to the usability and efficiency related to the probabilistic approach.

In particular, the future development of the project must address the following matters:

- improvement of the Ghosh's regression model in order to better grasp the intensity peaks neglected by the current method;
- joint consideration in the same framework of main-shocks and after-shocks scenarios.
- development of a model that may virtually account for the combination of seismic damage accumulation with aging and other non-seismic degradation phenomena.

The ultimate ambition of this work would be to lay the foundations for an integrated and planned development of the aforementioned topics so that the assessment of seismic risk is a valuable aid for the most current applications of civil engineering. Therefore, an at the forefront and multidisciplinary approach, continually supported by scientific research, is essential for responsible management of the seismic problem.

BIBLIOGRAPHY

- Bosco, F. (2014). IMPROVEMENT OF THE MODEL PROPOSED BY MENEGOTTO AND PINTO FOR STEEL.
- Debarati Datta, S. G. (2008). ESTIMATING PARK-ANG DAMAGE INDEX USING EQUIVALENT SYSTEMS. *World Conference on Earthquake Engineering* . Beijing.
- Freddi. (2016). Probabilistic Seismic Demand Modeling of Local Level Response Parameters of an RC Frame. *Earthquake Bulletin*.
- Freddi, F. (2012). *Local engineering demand parameters for seismic risk evaluation of low ductility reinforced concrete buildings*.
- Iunio Iervolino, M. G. (2015). Markovian modeling of seismic damage accumulation. *EARTHQUAKE ENGINEERING & STRUCTURAL DYNAMICS*.
- J. Ghosh, J. P.-S. (2015). Seismic Damage Accumulation in Highway Bridges in Earthquake-Prone Regions. *Earthquake Spectra*, 115–135.
- Kashani. (2016). Nonlinear fibre element modelling of RC bridge piers considering inelastic buckling of reinforcement. *Elsevier*.
- Kashani MM, B. A. (2015). “Influence of inelastic buckling on low-cycle fatigue degradation of reinforcing bars”. . *Constr Build Mater* , 94:644–655.
- Kashani, M. (2017). Influence of non-stationary content of ground-motions. *Bull Earthquake Eng*.
- Krawinkler, H. (1999). Challenges and progress in performance-based earthquake engineering. . *International Seminar on Seismic Engineering for Tomorrow*.
- Lehman DE, M. J. (2000). Seismic performance of well-confined concrete bridge columns. . *Pacific Earthquake Engineering Research Centre, Berkeley*.
- Mander JB, P. M. (1988). Theoretical stress–strain model for confined concrete. . *J Struct Eng* 1988;, 114(8):1804–25.
- Moehle, L. a. (2000). Seismic Performance of Well-Confined Concrete Bridge Columns. *Pacific Earthquake Engineering Research Center*.
- Park, Y. a.-S. (1985.). Mechanistic seismic damage model for reinforced concrete. *Journal of Structural Engineering*, 722–739.
- Popovics. (1988;). A numerical approach to the complete stress strain curve for concrete. *Cem Concr Res*, 3(5):583–99.
- Tubaldi, D. S. (2017). Effect of the damper property variability on the seismic reliability of linear systems equipped with viscous dampers. *Bull Earthquake Eng*.

